Ital. J. Geosci., Vol. 140, No. 3 (2021), pp. ..., 12 figs., 2 tabs. (https://doi.org/10.3301/IJG.2021.05)

Refining the middle-late Pleistocene chronology of marine terraces and uplift history in a sector of the Apulian foreland (southern Italy) by applying a synchronous correlation technique and amino acid racemization to *Patella* spp. and *Thetystrombus latus*

Vincenzo De Santis (1), Giovanni Scardino (1), Marco Meschis (2), José E. Ortiz (3), Yolanda Sánchez-Palencia (3) & Massimo Caldara (1)

ABSTRACT

For the first time, the synchronous correlation technique and amino acid racemization (AAR) analyses of *Patella* spp. and *Thetystrombus latus* shells are applied to an understudied sequence of raised palaeoshorelines to refine the knowledge about terrace phases and uplift history in the middle-late Pleistocene in a sector of the Apulian foreland (western coast of the Salento Peninsula, southern Italy). These combined methodologies provide the first chronological attribution for middle-late Pleistocene palaeoshorelines and quantitative assessment of vertical crustal movements in this sector of the Apulian foreland, which, to date, has been characterised by a scarcity of reliable chronological data.

By applying a synchronous correlation technique driven by new AAR analyses, we iterate different uplift rate scenarios to find the best match between digital terrain model and field-based observed palaeoshorelines and "expected" sea level highstand elevations.

Our results show that two uplift rate scenarios could explain the mapped geomorphology: (i) scenario 1 suggests fluctuating uplift rates over time with an uplift rate of 0.15 mm/y until 130 ky BP (middle Pleistocene, interval MIS 15 - MIS 6; that is, 590 - 130 ky BP) and of 0.07 mm/y from 130 ky BP to the present; on the other hand, (ii) scenario 2 suggests a constant uplift rate of 0.12 mm/y over time in the middle-late Pleistocene.

The palaeoshorelines recognised in this study are related to the following highstands: 119 ky BP (MIS 5.5 second peak), 125 ky BP (MIS 5.5), 240 ky BP (MIS 7.5), 340 ky BP (MIS 9.3), and 478 ky BP (MIS 13.1) for both scenarios 1 and 2. The two scenarios only differ in the oldest palaeoshoreline: 560 ky BP (MIS 15.3) in scenario 1 and 550 ky BP (MIS 15.1) in scenario 2.

Our results highlight how the number of preserved palaeoshorelines is controlled by uplift rates; indeed, in this area, we show that fewer palaeoshorelines are preserved than in regions where higher uplift rates have been inferred, suggesting a more prominent effect of the "overprinting" or re-occupation of younger sea level highstands over the older sea level highstands. Finally, we discuss geomorphological and geological implications of using a synchronous correlation approach, driven by new age controls, to model raised palaeoshorelines where relatively low uplift rates have been mapped within well-known geodynamically stable regions, such as the Apulian foreland, southern Italy.

Key words: synchronous correlation technique, amino acid racemization on *Patella* spp. and *Thetystrombus latus*, terrace phases, Apulian foreland, overprinting and re-occupation.

(1) Dipartimento di Scienze della Terra e Geoambientali, Università degli Studi di Bari "Aldo Moro", Via Orabona 4, 70125 Bari, Italy.
(2) Dipartimento di Fisica e Astronomia, Università di Bologna, Via Carlo Berti Pichat, 8, 40127, Bologna (Italy).
(3) Biomolecular Stratigraphy Laboratory, Madrid School of Mines, C/Rios Rosas 21, E-28003 Madrid, Spain.
Corresponding author e-mail: vincenzo.desantis@uniba.it

INTRODUCTION

Marine terraces are widespread features that occur due to the interaction between sea-level oscillations and vertical land movements (Bloom, 1980; Murray-Wallace & Woodroffe, 2014; Grant *et alii*, 2014; Marra *et alii*, 2019). The study of these landforms is fundamental for the assessment of past sea-level changes and vertical land movements, in that their current elevations provide an estimation of crustal uplift or subsidence rates (e.g., Ferranti *et alii*, 2006; Caputo *et alii*, 2010; Meschis *et alii*, 2020).

The study area lies within the Apulian foreland, particularly within the Salento highlands. The Apulian foreland belongs to a zone of active convergence where Quaternary uplift is evidenced by a well-exposed sequence of raised marine terraces. The complexity of deformation in regions that, such as the Apulian foreland, are subject to a combination of deformative processes leads to uncertainty in the quantification of their role in the geodynamics of foreland regions.

Although the extensive presence of marine terraces has been documented throughout the central southern Apulian foreland, that is, in the Murge and Salento highlands (Ciaranfi *et alii*, 1992), there are few chronological constraints regarding them.

Indeed, there are several difficulties in the development of a chronology of terrace formation in the area of the Apulian foreland, such as scarcity of outcrops of terrace deposits and datable sedimentary material and very small thicknesses of deposits. As a result, to date, acknowledgement of a well-constrained chronology of marine terraces linked to glacio-eustatic oscillations is still debated in the study area. For this reason, an in-depth study of uplifted marine terraces and their related sedimentary deposits was performed in the coastal sector north of Gallipoli city (Figure 1) to provide new insights into its morpho-topography and chronology. Our study aims to (i) map the palaeoshoreline elevations, (ii) provide new refined ages for undated palaeoshorelines and, as a consequence, (iii) refine the chronology and spatial extent of uplift. This was accomplished by applying the synchronous correlation technique (Roberts *et alii*, 2009, 2013; Meschis *et alii*, 2018, 2020; Robertson *et alii*, 2019) driven by new amino acid racemization (AAR) analyses.

GEOLOGICAL SETTING AND PREVIOUS RESEARCH

From the Late Triassic to Cretaceous, a subsiding carbonate platform (Apulian platform; D'Argenio, 1974) was established on the southern edge of the expanding Tethys Ocean (van Hinsbergen *et alii*, 2014, 2020), which produced a thick succession of Mesozoic limestones, now cropping out extensively throughout the Apulia region (Ricchetti *et alii*, 1992).

Since the middle Miocene, the Apulian platform has played the role of foreland in both the east-verging Apennine and west-verging Dinaric orogens (Ricchetti *et alii*, 1992) and has been affected by two opposite-verging tectonic thrust processes (Ricchetti & Mongelli, 1980; Doglioni *et alii*, 1994, 1996). At the present, the Apulia region is characterised by three main geographic domains, Promontorio del Gargano, Murge highlands, and Serre Salentine, which are separated by the structural and morphological grabens formed by the Tavoliere di Puglia and Tavoliere di Lecce plains (Fig. 1A). During the Plio-Pleistocene, two geodynamic phases affected the Apulian foreland (Ricchetti *et alii*, 1992). In the first phase, the extreme western sectors of the Apulian foreland underwent strong subsidence (Doglioni *et alii*, 1994) because of subduction beneath the Apennine chain. Thus, wide sectors of foreland evolved into a foredeep (Bradanic Trough). In this context, the Bradanic Trough sedimentary cycle (Ricchetti *et alii*, 1992; Tropeano *et alii*, 2002) began to accumulate coastal deposits belonging to Calcarenite di Gravina (GRA; Azzaroli, 1968; Iannone & Pieri, 1979), which culminated in silty clay hemipelagic deposits belonging to Argille subappennine (ASP; Azzaroli *et alii*, 1968). In the second geodynamic phase (from the middle Pleistocene), the entire Apulian foreland and Bradanic Trough were uplifted (Ricchetti *et alii*, 1992; Doglioni *et alii*, 1994, 1996); the regressive deposits of the Bradanic Trough cycle and/or the marine and continental terrace deposits confirm this process (Ciaranfi *et alii*, 1992). Glacio-eustatic sea level oscillations occurred concurrently with the regional uplift, which affected regression. The glacio-eustatic oscillations also contributed to the deepening of karst valleys (locally called lame) that characterise the Murgian karst plateau and of the incised valleys recognised on the Apulian continental shelf (De Santis & Caldara, 2016; De Santis *et alii*, 2020a, 2020b; Valenzano *et alii*, 2018).

To date, the Apulian foreland has been characterised by a scarcity of reliable chronological data concerning the phases of marine terracing and the vertical displacement of the palaeoshorelines during the middle-late Pleistocene (Cerrone *et alii*, in press).

Indeed, for this period, the most numerous and well chronologically constrained data are only those related to marine terrace deposits of the Tavoliere di Puglia plain (De Santis *et alii*, 2010, 2013, 2014a), Trani cliff (Caldara *et alii*, 2013; De Santis *et alii*, 2014b), and Apulian Ionian coast between Taranto and the border with the Basilicata region, represented by the Bradano River (Brückner, 1980; Boenzi *et alii*, 1986; Belluomini *et alii*, 2002; Zander *et alii*, 2006; Amorosi *et alii*, 2014; De Santis *et alii*, 2018, 2020c).

Along the Ionian coast between Taranto and Santa Maria di Leuca, chronological constraints are available but these are related to the deposits of MIS 5.5 sea level highstand confirmed by the presence of the so-called "*Senegalensis* fauna", mapped at different topographic elevations between the present sea level and 26 m above the present sea level (a.p.s.l), with the presence of *Thetystrombus latus* (sin.: *Strombus bubonius)* (Hearty & Dai Pra, 1992; Belluomini *et alii*, 2002, Caldara *et alii*, 2003; Amorosi *et alii*, 2014; Negri *et alii*, 2015).

In particular, in the area near Gallipoli town, the most studied sites close to our study area are: Torre Castiglione (immediately north of our study area), Torre Sabea and Ospedale di Gallipoli (immediately south of our study area). These three sites are reported respectively with id numbers 10, 11, and 12 in Hearty & Dai Pra, 1992). At Torre Castiglione, three marine deposits lie in superposition, separated by unconformities and discontinuous, thin soils:

1) Unit MV (with subunits MVa and MVb). Subunit MVa is a light grey algal calcarenite with vacuolar structure (fenestrae) rich in Astraea rugosa. The age of this subunit is greater than 300 ka (Dai Pra & Stearns, 1977). Subunit MVb is a yellowish, medium-grained bioclastic calcarenite, rich in Cladocora caespitosa in growth position.
2) Unit MIV is composed of detrital organogenic limestones, and a clayey-marl matrix rich in embedded organic remnants of a pale brown soil with root and burrow-casts; this unit has been attributed to Aminozone F (MIS 7; Hearty & Dai Pra, 1992)
3) Unit MIII is unconformable on Unit IV and consists of bioclastic limestone with a micritic matrix. *Lithothamnium* and intraclasts are common. The fauna displays ecological diversity and includes *Cladocora*, *Spondylus*, *Conus*, *Glycymeris*, *Arca*, *Thetystrombus latus*.
4) Unit MII is a younger marine calcarenite contains reworked, rounded intraclasts of older units.

At Torre Sabea, the last interglacial sea level incised a small terrace at about 1 m into MV unit. The MIII unit is near sea level and consists of calcarenite with *Thetystrombus latus* which grades upward and laterally into an eolianite (unit DIII) of the back beach zone. Unit MIII at Torre Sabea has been attributed to Aminozone E (MIS 5.5; Hearty & Dai Pra, 1992). Units MIII-DIII are truncated, and overlain by a thin soil (SIII) and capped by another eolianite (unit DIIIb) for which equivalent marine facies is not observed above sea level. Another thin soil (SII) separates the lower Pleistocene deposits from the DI eolianite capping the section; this latter eolianite at Torre Sabea has been attributed to Aminozone A (Holocene; Hearty & Dai Pra, 1992).

At Ospedale di Gallipoli, apparently several marine deposits containing *Thetystrombus latus* can be observed; unit MIII appear to be separated into two sub-units: a thin soil (unit SIII) separates the lower planar beds of the shoreface (subunit MIIIa) from an upper zone with highly concentrated shells (subunit MIIIb) and *Thetystrombus latus*. Notwithstanding the difficulties in interpreting the stratigraphy of this site, Hearty & Dai Pra (1985) determined that all of the deposits are essentially the same age, and both subunits MIIIa and MIIIb have been attributed to Aminozone E (MIS 5.5; Hearty & Dai Pra, 1992). The thin, weakly-developed "soil" (unit SIII) may either be penecontemporaneous with the beach deposits as a backbeach "protosol" which was buried by marine deposits during storms, or, the soil may represent

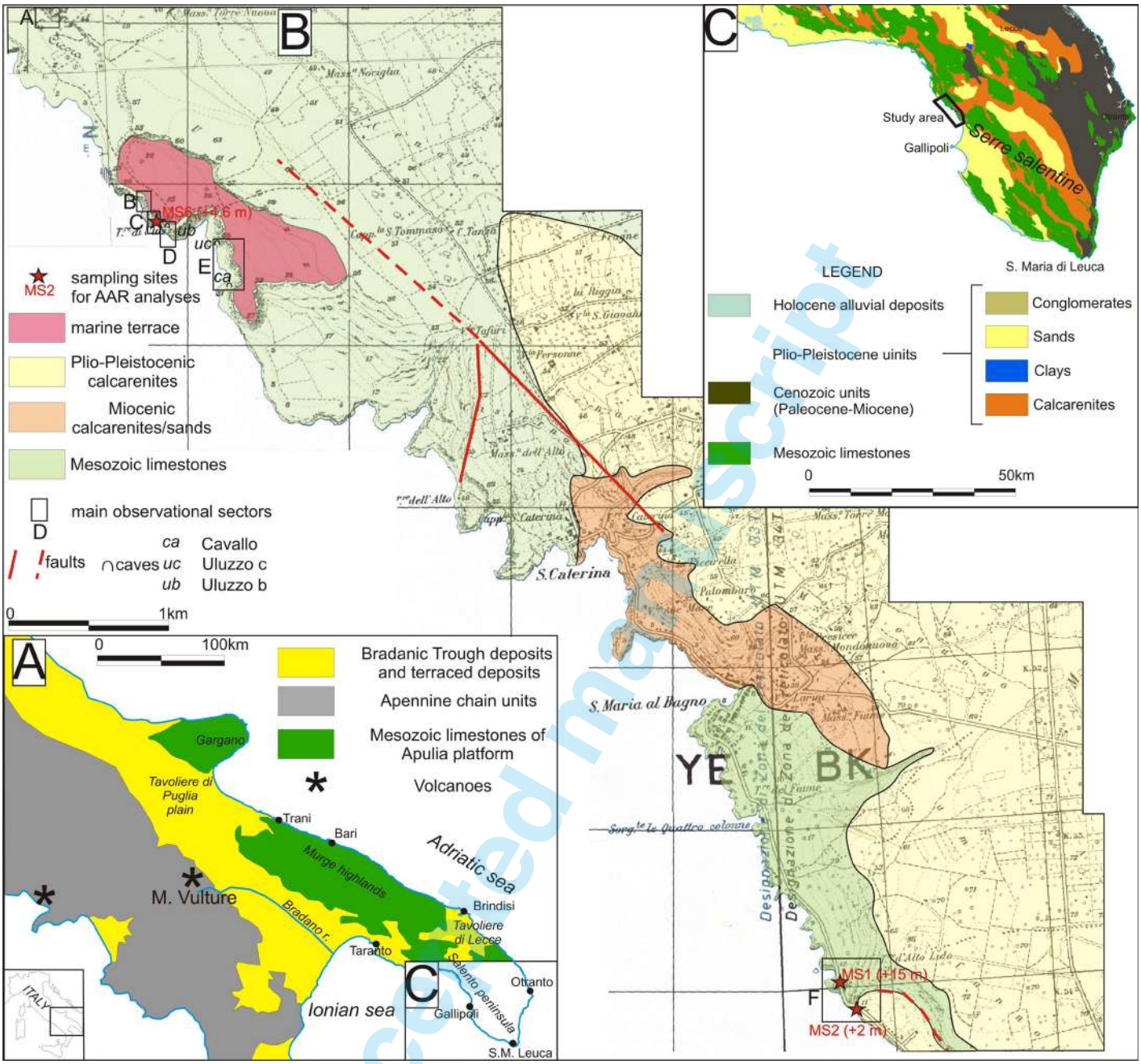

Fig. 1 - Study area. A: Regional context showing the main geological-structural domains in southern Italy. B: Detail (on 1:25.000 scale base map) of Italian official geological map (Largaiolli et alii, 1969), which shows the main sectors (capital letters from A to F) from which photographs of palaeoshorelines described in this paper were taken; sector A (La Cicora locality); sectors B, C, D, E (Uluzzo locality); sector F (Montagna Spaccata-Torre d'Alto Lido locality). Note that in this map the informal terraced units recognised in this work have not been reported because of they crop out in very small and scattered patches and the precise cartography of the terraced units was beyond the main purpose of this work C: Simplified geological map of the Salento Peninsula (from Boenzi et alii, 2010), showing in particular the structural tectonic setup defined as "Serre salentine": a series of horsts and grabens elongated in a NW-SE direction.

interglacial sea-level oscillations. A stratigraphy reflecting such oscillations of sea level during the last interglacial period (Stage 5e) has been described in other localities in Italy (Hearty & Dai Pra, 1987), Mallorca (Hearty, 1987), Spain (Hearty *et alii*, 1987), Tunisia (Hearty, 1986).

Along the Ionian coast from the city of Taranto and Bradano River, which marks the border between the Apulia and Basilicata regions, Boenzi *et alii* (1986) recognised MIS 5.5 deposits with *Thetystrombus latus* near the Castellaneta marina locality, while De Santis *et alii* (2018, 2020c) recognised and mapped three terrace deposits that date to MIS 7.3, MIS 7.1, and MIS 5 highstands.

The few data available along the Adriatic coast (Mastronuzzi *et alii*, 2011; De Giosa *et alii*, 2019) are rare, mostly poorly chronologically constrained and refer exclusively to marine terraced deposits attributed to MIS 5.5 because there are no well-exposed outcrops, and even those related to MIS 5.5 are more difficult to recognise in the field due to the absence of "*Senegalensis* fauna", which probably never colonised this coastal stretch during the last interglacial period.

A few exceptions are represented by the Trani cliff, where Caldara *et alii* (2013) and De Santis *et alii* (2014b) described some Quaternary units attributed by the authors to MIS 9, MIS 8.5 and MIS 7.1.

One indirect age constraint is also available at the Santa Sabina locality, ca. 24 km north of Brindisi, where a coastal deposit at approximately 3 m a.p.s.l. overlies a colluvial deposit bearing late Palaeolithic-Mousterian flints and, thus, could be of MIS 5.5 age (Mastronuzzi & Sansò, 2003; Marsico *et alii*, 2003). Geochronological data constrained the occurrence of MIS 5 between Capo Santa Maria di Leuca and Otranto at approximately 6 m a.p.s.l. (Ferranti *et alii* 2006; Mastronuzzi *et alii*, 2007; Sansò *et aliii*, 2015).

As a consequence of this knowledge framework on marine terraces of the middle-late Pleistocene, to date, most uplift rates of the Apulian foreland have been estimated only for the late Pleistocene almost exclusively along the Ionian coast by means of the elevation of the marine terrace deposits related to the last interglacial period (MIS 5.5) (Hearty & Dai Pra, 1992; Belluomini *et alii*, 2002; Ferranti *et alii*, 2006). Furthermore, these data show a decreasing uplift rate from the northwest to southeast, such as 0.31 mm/y northwest of Taranto (Ponte del Re locality), 0.18 mm/y around Taranto (Santa Teresiola and Masseria San Pietro localities), 0.11 mm/y at Torre Colimena, –0.03 mm/y at Torre Castiglione, 0.03 mm/y at Gallipoli, and 0.02 mm/y at Torre San Giovanni (Mastronuzzi *et alii*, 2007). Uplift rates along the eastern side of the Apulian foreland (Adriatic coast) are more difficult to determine with reliable chronological constraints.

Geological background of the study area

The study area consists of a coastal stretch, ca. 7 km long (Fig. 1B), located along the Ionian coast of the Salento Peninsula, which forms the southern portion of the Apulian foreland. The structural setup of the Salento Peninsula is defined as the "Serre salentine" domain and consists of a series of horsts and grabens elongated NW-SE (Ricchetti & Ciaranfi, 2013; Fig. 1C); the horsts, whose surfaces are flat and slightly tilted towards the SW, consist of Mesozoic or Palaeogene-Miocene carbonate units; the grabens, on the other hand, contain Plio-Pleistocene terrigenous deposits belonging to the Bradanic trough cycle or to the subsequent marine terrace deposits connected to the regional tectonic uplift.

The study area, located just north of the city of Gallipoli (Fig. 1C), coincides with most of its extension with the western slope of one of the NW-SE oriented horsts that characterises the Salento Peninsula.

This area also represents one of the few coastal stretches with high and rocky coasts on the entire Apulian Ionian side. Furthermore, because of the still relatively low anthropization (the study area is located in the natural reserve of Porto Selvaggio), it is easier to find traces of palaeoshorelines.

In the adjacent coastal stretches, the morphology is instead characterised by very low slopes and extensive anthropization, both urban and agricultural, a feature that makes it difficult to recognise palaeoshorelines in the field, which, moreover, due to the low gradient, are located much further from the coast than in our study area.

From a geological point of view, the study area is characterised almost exclusively by outcrops of Mesozoic limestone (Fig. 1B), with small patches of marine terrace deposits, never mapped thus far. Only in the coastal stretch between Santa Caterina and Santa Maria al Bagno calcarenites and sands crop out (Fig. 1B), and these are attributed to the Miocene (Calcareniti di Andrano; Largaiolli *et alii*, 1969; Boenzi *et alii*, 2010), while in the inner, central-southern belt of the study area, Plio-Pleistocene calcarenites crop out (Largaiolli *et alii*, 1969).

In the study area, many caves are present, among which Grotta Uluzzo B, Grotta Uluzzo C, and Grotta del Cavallo (Fig. 1; Fiorini *et alii*, 2019), which are very important sites for the so-called "Uluzzian", had a distinctive culture characterising the Middle-Upper Palaeolithic transition in Italy (Boscato & Crezzini, 2012).

METHODS

Field survey and Digital Terrain Model (DTM)

We mapped palaeoshorelines and collected their elevations above present sea level through a combination of an intensive field survey and a 2-m digital terrain model (DTM) extracted by high-resolution light detection and ranging (LiDAR) provided by "Ministero dell'Ambiente e della Tutela del Territorio e del Mare" (Fig. 2). Elevations of palaeoshorelines were obtained using a Global Position System Real-Time Kinematic (GPS-RTK) receiver. The permanent stations of the Global Navigation Satellite System (GNSS), sited in the Apulia region (gps.sit.puglia.it), were used to improve the accuracy of the GPS-RTK receiver, dependent on ionospheric and tropospheric delays and uncertainties in the sources of satellite clocks. For each measurement performed, the accuracy of the GPS-RTK receiver ranged between 0.05 and 0.1 m.

A survey with total stations was performed to assess the altitudes of the palaeoshorelines located on the very steep slopes, where it was difficult to use the GPS-RTK receiver. The accuracy of the total station ranged between 0.001 and 0.005 m, dependent on atmospheric perturbations. Field geomorphological indicators used to identify palaeoshorelines include inner edges, notches, caves, bands of lithophagid borings, marine deposits on wave-cut platforms including coarse sands, algal reefs, conglomerates with lithophagids and sponge-bored pebbles (Ferranti *et alii*, 2006; Vacchi *et alii*, 2016).

The error related to the paleo-shoreline mapped in the field is prominently linked to the uncertainty of annexed markers.

For the lithophagid borings, the error was assumed to be equal to ± 2 m at the upper limit, considering that they colonize down to deeper than 30 m below the sea-level of calcareous rocky coasts and can be detected up to 2 m below sea-level (Pirazzoli *et alii*, 1999; Ferranti *et alii*, 2006). However, if the upper limit of *Lithophaga* populations is clearly visible and well determined, it can represent a good sea-level indicator (Evelpidou *et alii*, 2012).

The error linked to the tidal notches in the Mediterranean is dependent on the local tide phases, which for this area is of about 0.4 m (Antonioli et *alii*, 2015, 2018). The base of a tidal notch is considered the

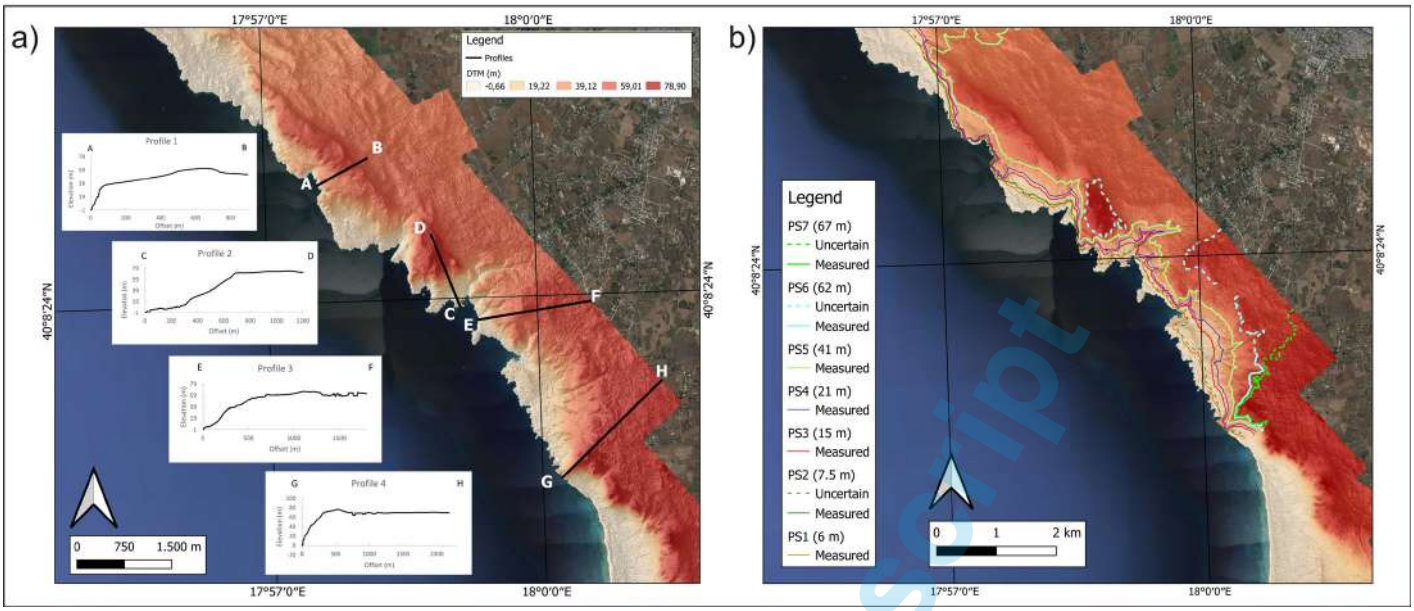

Fig. 2 - Two m digital terrain model (DTM) of the study area with the four topographic profiles extracted (a) and coloured lines that represent the mapped palaeoshorelines (b).

best and most precise marker of average palaeo-sea level because its width is closely linked to the local tidal phase (Antonioli *et alii*, 2015; Rovere *et alii*, 2016; Lorscheid *et alii*, 2017).

The errors linked to the palaeo-beaches were considered in relation to the *Thetystrombus latus* and senegalensis fauna occurrence (indicative of MIS 5.5) (Gignoux, 1913; Zazo *et alii*, 2003; Taviani, 2014; Benjamin *et alii*, 2017). The elevation of beach facies with the presence of *Tethystrombus latus* and senegalensis fauna is a useful marker of the palaeo beach deposits (Benjamin *et alii*, 2017), with an error of ± 0.5 m for Gallipoli area, dependent on the GPS – RTK resolution and tide phase.

Amino Acid racemization analyses (AAR) on *Patella* sp. and *Thetystrombus latus*

Chronological analyses were performed by applying amino acid racemisation (AAR) to shells of *Patella aspera* (Röding), *Patella caerulea* Linneo, *Patella* sp. and *Thetystrombus latus* (Gmelin) found in deposits associated with two palaeoshorelines: eight *Patella* spp. samples collected from a deposit located at +15 m (sampling site MS1; Fig. 1), two *Thetystrombus latus* (Gmelin) samples collected from a deposit located at +2 m (sampling site MS2; Fig. 1), and three *Patella* spp. samples collected from a deposit located at +4.6 (sampling site MS6; Fig. 1) were analysed in the Biomolecular Stratigraphy Laboratory of the Polytechnical University of Madrid.

Several studies have demonstrated that *Patella* shells are satisfactory materials for amino acid racemization dating of palaeontological and archaeological sites (Ortiz *et alii*, 2009, 2015; Demarchi *et alii*, 2011, 2013a, b). Furthermore, it must be considered that many results of AAR analyses carried out on *Patella* sp. have been confirmed in field by other chronological constraint obtained on the same deposits containing this taxon; in particular, similar results were obtained both from other organisms considered more reliable for the AAR method (eg *Glycymeris sp.*) and from other independent dating methods (Torres *et alii*, 2000; 2010).

For AAR, a hollow diamond drill was used to remove a discoid sample (8 mm in diameter) from the apex of the *Patella* spp. shells. Discoid samples were also collected from the columella of *Thetystrombus latus* (Gmelin). Peripheral parts (approximately 20-30%) were removed after chemical etching with 2 N HCl. Afterwards, 10-20 mg of sample was collected.

Amino acid concentrations were quantified using HPLC following the sample preparation protocol described in Kaufman & Manley (1998) and Kaufman (2000). This procedure involves hydrolysis, which was performed under a N_2 atmosphere in 20 µl/mg 7 M HCl. The hydrolysates were evaporated to dryness in vacuo and then rehydrated in 10 µl/mg 0.01 M HCl with 1.5 mM sodium azide and 0.03 mM L-homo-arginine (internal standard).

Samples were injected into an Agilent HPLC-1100 equipped with a fluorescence detector. Excitation and emission wavelengths were programmed at 335 nm and 445, respectively. A Hypersil BDS C18 reverse-phase column (5 µm; 250 x 4 mm i.d.) was used for the analysis.

Derivatization occurred before injection by mixing the sample (2 µl) with the precolumn derivatization reagent (2.2 µl), which comprised 260 mM isobutyryl-L-cysteine (chiral thiol) and 170 mM o-phthaldialdehyde, dissolved in 1.0 M potassium borate buffer solution at pH 10.4. Eluent A consisted of 23 mM sodium acetate with 1.5 mM sodium azide and 1.3 microM EDTA, adjusted to pH 6.00 with 10 M sodium hydroxide and 10% acetic acid. Eluent B was HPLC-grade methanol, and eluent C consisted of HPLC-grade acetonitrile. A linear gradient was performed at 1.0 ml/min and 25°C, from 95% eluent A and 5% eluent B upon injection to 76.6 eluent A, 23% eluent B, and 0.4% eluent C at min 31.

Synchronous correlation technique to model multiple sea level highstands and multiple palaeoshorelines

In this work, we do not correlate a single palaeoshoreline with a sea-level highstand and then the next higher palaeoshoreline with the next older highstand, but we apply a synchronous correlation technique which crosses one or more uplift rates over time with sea level highstands. This technique has been used by previous investigations within the Mediterranean realm and elsewhere (Roberts *et alii*, 2009, 2013; Meschis *et alii*, 2018, 2020; Pedoja *et alii*, 2018; Robertson *et alii*, 2019). This approach is based on the assumption that sea level highstands are unevenly spaced in time, implying that for a constant uplift rate over a time interval, uplifted palaeoshorelines are unevenly spaced in elevation.

It is important to note that it is crucial to obtain at least one chronological constraint for a palaeoshoreline across the investigated topographic transects. Indeed, the age constraint drives the iteration of the uplift rate to the entire topographic transect, synchronously modelling all mapped palaeoshorelines. Furthermore, this technique tests whether undated palaeoshorelines can be modelled by iterated uplift rates implied by chronologically constrained palaeoshoreline(s). To iterate different uplift rate scenarios, we use a "Terrace Calculator" built in Excel, where sea level highstands are entered (Roberts *et alii,* 2013; Robertson *et alii,* 2019). This approach forces the user to maximise the coefficient of determination (R^2 value) for linear regression analysis through data including the "measured" elevations and the "expected" elevations of all palaeoshorelines on a topographic profile. The "expected" palaeoshoreline elevations represent the present sea level highstand elevations derived by iterating uplift rate values driven by age constraints and using well-known sea level curves for the last 1 My (Siddall *et alii*, 2003; Rohling *et alii*, 2014). We adopted the results from sea level curves of Siddall *et alii* (2003) until 410 ky and Rohling *et alii* (2014) after 410 ky, which have already proven suitable for reproducing the geomorphology of marine terraces in the Mediterranean region (Roberts *et alii*, 2009, 2013; Meschis *et alii*, 2018, 2020; Robertson *et alii*, 2019).

Note that for this study, also other sea level curves were tested (Waelbroeck *et alii*, 2002; Grant *et alii*, 2014), but they gave results less congruent with what was observed on field.

Regarding the sea level curve of Siddall *et alii* (2003), the reported uncertainty in sea level is 12 m, while the uncertainty in age highstands is not defined. Concerning the sea level curve of Rohling *et alii* (2014), the reported uncertainty in sea level is 6 m, while the uncertainty in the age of sea level highstands is reported to be 4 kyr. This technique uses an input uplift rate (UR), which is iterated to calculate the predicted elevations (PE) of all sea-level highstands using the age of the highstands (T) and the sea level elevations of the highstands relative to the sea level of today (SLT) following this formula: PE = (UR x T) + SLT.

For our study, two uplift rate scenarios are supported, showing the best match between expected and observed palaeoshoreline elevations.

Scenario 1 (two uplift rates) involves:

a) An uplift rate for part of the middle Pleistocene (MIS 15 - MIS 6, that is, 590 - 130 ky BP), which is derived by the iteration of unique uplift rates until finding the one that offers the best match between expected and observed palaeoshoreline (see the DATA and RESULTS section).
b) A different uplift rate starting from the late Pleistocene (MIS 5 - onwards, that is, from 130 ky BP onwards), which derives from a field interpretation of the AAR results regarding a palaeoshoreline at +15 m (see the DATA and RESULTS sections).

Scenario 2 (a single constant uplift rate) involves a unique uplift rate that also takes into account the results of the AAR analysis without specific interpretations.

The output of the terrace calculator is a set of expected elevations for sea level highstands (that is, expected palaeoshoreline elevations); we consider acceptable a difference between expected and observed palaeoshoreline elevations up to 10 m based on the uncertainties of the sea level curve used regarding both the sea level and age of highstands. If this is the case, we assign our observed palaeoshorelines to expected highstands.

DATA AND RESULTS

Palaeoshorelines recognised in the field

A detailed field survey of the study area reveals prominent palaeoshoreline features cut into Mesozoic bedrock, including bands of lithophagid borings (especially *Gastrochaenolites torpedo* Kelly & Bromley due to *Lithophaga lithophaga* (Linneo)), inner edges, residual tidal notches, sea caves, and syn-wave-cut platform deposits.

The common feature of all identified palaeoshorelines is that they can be observed at the same elevation throughout the study area. Below, we list the identified palaeoshorelines in the field, referring to six key sectors (Fig. 1B) for their observation: from N to S, sector A (La Cicora locality), sectors B, C, D, E (Uluzzo locality); sector F (Montagna Spaccata-Torre d'Alto Lido locality).

1) Palaeoshoreline PS1 and Unit I (elevation: ~ +6). This palaeoshoreline (Fig. 3) is represented by a band of lithophagid borings in Mesozoic limestones; PS1 is the palaeoshoreline that has the greatest lateral continuity and is characterised by a progressive growth in the density of borings up to an upper band that has the highest density in the entire study area; the upper limit of this band of maximum density of borings varies between +4 and +6 metres above the present sea level (hereinafter: m. a.p.s.l.). This band of lithophagid borings whose upper limit oscillates between +4 and +6 m was considered to be indicative of a palaeoshoreline at +6 m, since from the upper limit of the lithophagid band, a subhorizontal line is defined, which is considered a reliable marker of a past mean sea-level position (Ferranti *et alii*, 2006; Stiros *et alii*, 1992).

PS1 is associated with a greyish to reddish, well-cemented limestone-calciruditic deposit rich in bioclasts (Unit I) and transgressive on the Mesozoic limestone basement. Unit I has its highest point of outcrop exactly coinciding with the upper limit of the band of maximum density of borings, following its oscillations between +4 and +6 m. a.p.s.l. Unit I contains, among others, specimens of *Patella* sp., *P. caerulea* Linneo, *Bolma rugosa* (Linneo), *Cerithium lividulum* Risso, *Melarhaphe neritoides* (Linneo), *Gibbula*

Fig. 3 - Field photographs of PS1; the top left capital letters indicate the sector of observation (see Fig. 1). The upper limit of the band of lithophagid borings is indicated by black arrows; note the upper boundary of greysh deposits of Unit I, which follows the course of the band of lithophagid borings. Black horizontal lines with elevations in metres above the present sea level are indicated.

sp., *Murex* sp., *Columbella rustica* (Linneo), *Truncullariopsis trunculus* (Linneo), *Barbatia barbata* (Linneo), *Spondylus gaederopus* Linneo, *Clanculus corallinus* (Gmelin), *Striarca lactea* (Linneo), *Chlamys* sp., *Mytilus* sp., and *Arca* sp. The upper limit of the band of lithophagid borings, as well as the associated upper limit of Unit I, can be observed ca. + 4 m in sector B (Fig. 3B); between +5 and + 6 m in sectors C (where the MS6 sampling site is located; Figs. 1 and 3C; Table 1) and D (Fig. 3D), and between +4.5 and +5.8 m in sector E (Fig. 3E). In sector F, the upper limit of the band of lithophagid borings can be observed at approximately +4.5 m (Fig. 3F), and the associated Unit I also contains *Thetystrombus latus* (Gmelin) and *Cladocora caespitosa* Linneo, observable ca. +2 m. a.p.s.l. (MS2 sampling site; Fig. 1, Table 1).

2) Palaeoshoreline PS2 (elevation: ~ +7.5). This palaeoshoreline is represented by a band of lithophagid borings grouped in discontinuous clusters within Mesozoic limestones whose upper limit is ca. + 7.5 m. a.p.s.l. (Fig. 4).

Sometimes, this palaeoshoreline appears well separated from the previous palaeoshoreline, and sometimes there

Fig. 4 - Field photographs of PS2. The top left capital letters indicate the sector of observation (see Fig. 1); the black arrows indicate lithophagid borings. Black horizontal lines with elevations in metres above the present sea level are indicated

are also scattered lithophagid borings in the Mesozoic limestone interposed between palaeoshorelines PS1 and PS2.

PS2 is mainly visible in sectors B, D, and E (Fig. 4 B, D, and E); it is also recognisable but less evident in sector F. In sectors B and D, PS2 is associated with a cemented coarse calciruditic deposit, with a reddish matrix composed of calcarenite/calcisiltite (Unit II); this deposit is transgressive on the Mesozoic limestone basement and has its highest outcrop point just below the discontinuous band of lithophagid borings, which represents PS2. The stratigraphic relationship between Units II and I is not easily deduced in the field; Unit II probably underlies Unit I, but we do not exclude a partial lateral transition between the two units.

The macrofauna of Unit II is not widespread throughout the unit but is localised in clusters where the following specimens have been recognised: *Bolma rugosa* (Linneo), *Trunculariopsis trunculus* (Linneo), *Cerithium* sp., *Clanculus corallinus* (Gmelin), *Striarca lactea* (Linneo), *Spondylus gaederopus* Linneo, *Mytilus* sp., and *Arca* sp.

3) Palaeoshoreline PS3 (elevation: ~ 15). This palaeoshoreline is sometimes represented by a band of lithophagid borings grouped in discontinuous clusters within Mesozoic limestones whose upper limit is ca. +15 m. a.p.s.l.; sometimes by residual tidal notches or inner edges incised into the Mesozoic limestones (Fig. 5). PS3 is mainly visible in sectors A, E, and F. At only one point, in sector E, the elevation of PS3 measured in the field was +16 m a.p.s.l. In sector A, it appears as a small subvertical slope, less than a metre high, with a very narrow abrasion platform in front, both incised into the Mesozoic limestones. On the slope, there is evidence of altered lithophagid borings; both the slope and platform are covered by continental deposits, consisting of limestone breccia in a reddish clayey-sandy matrix.

In sector E, PS3 is represented by a probable remnant of a tidal notch and, laterally to this, by a band of lithophagid borings grouped in discontinuous clusters whose upper limit is ca. +15 m. a.p.s.l (Fig. 5E). In sector F (called "Montagna Spaccata-Torre d'Alto Lido"), along the coastal road, PS3 is represented by a well-preserved inner edge with lithophagid borings, an associated wave-cut platform some metres wide (both carved into the Mesozoic limestones), and a syn-wave-cut platform deposit (Fig. 5F); this outcrop has already been described and interpreted by Palmentola & Lazzari (2005). The syn-wave-cut platform deposit (Unit III; MS1 sampling site (Fig. 1, Table 1)) is composed of pebbles in a coarse sandy matrix, algal calcarenite and mudstone with marine fossils, such as *Fissurella* sp., *Patella aspera* (Röding), *Patella caerulea* Linneo, *Tritia neritea* (Linneo), *Jujubinus* sp., *Gibbula* sp., *Clanculus cruciatus* Linneo, *C. corallinus* (Gmelin), *Bolma rugosa* (Linneo), *Tricola pullus* Risso, *Littorina* sp. Mitrella sp., *Cerithium lividulum* Risso, *Vermetus* sp., Spirorbidae spp., and *Cardita calyculata* Linneo. Continental reddish clinostratified coarse breccias (br in Fig. 5F), approximately 1.5 m thick, interbedded with reddish silty-sandy deposits cover all marine deposits.

4) Palaeoshoreline PS4 (elevation: ~ +21). This palaeoshoreline is represented by a band of lithophagid borings grouped in discontinuous clusters within Mesozoic limestones whose upper limit is ca. +21 m. a.p.s.l (Fig. 6). PS4 is mainly visible in sectors E and F. In sector E, this palaeoshoreline is represented by a small residual wave-cut platform, two sea caves, lithophagid borings, *Gastrochaenolites cor* Bromley & D'Alessandro with the original borer *Petricola lithophaga* (Retzius), and a small patch of a syn-wave-cut platform deposit (Unit IV; Fig. 6E) composed of well-cemented calcirudite. In sector F, this palaeoshoreline is represented by a band of lithophagid borings grouped in discontinuous clusters within Mesozoic limestones (Fig. 6F).

5) Palaeoshorelines PS5 (elevation: +41), PS6 (elevation: ~ +62), and PS7 (elevation: ~ +67). These three palaeoshorelines are described together because of the common characteristics that distinguish them. PS6 and PS7 were observed in the field only in sector F because here, the rocky slope reaches the higher elevation a.p.s.l. and it is sparsely vegetated. All these palaeoshorelines are represented by bands of lithophagid borings grouped in discontinuous clusters (Fig. 7); note that the elevations represent, as always, the points of maximum elevation of these bands above the present sea level.

Lithophagid borings are sometimes in Mesozoic limestones; sometimes instead, they are in deposits unconformably lying ontop Mesozoic limestones and consist of greyish cemented breccias with limestone clasts and scarce or no matrix or of reddish well-cemented pebbles in a sandy-clay matrix in which vertebrate teeth and bones can be seen. Given the scarcity of the outcrops of these deposits, they have not been described as real units, but only their presence is reported here.

Palaeoshorelines recognised in the DTM

The palaeoshorelines identified in the field are not always recognisable when geomorphic features are mapped using the detailed DTM in a geographic information system (GIS) environment (Fig. 2). This is also shown in the four DTM-based topographic profiles. This is because the coast consists of very compact and resistant Mesozoic limestones, which rarely allowed the creation of evident and deep abrasion platforms and associated cliffs at their inner edges. The only exception is PS6, which is associated with a small marine terrace in the northern part of the study area, behind sectors B, C, D, and E (Fig. 1B). As a consequence, the palaeoshorelines are often placed at a short distance from each other. This may lead to some difficulties when palaeoshorelines are tentatively mapped in the detailed DTM, especially if coupled with the fact that they contain bands of lithophagid borings, tidal notches and caves (Figs. 8, 9).

Furthermore, the presence of mass movements and related slope deposits on some parts in the coastal area can disturb the lateral continuity of the palaeoshorelines.

Amino Acid Racemization analyses

The mean D/L values of three amino acids (isoleucine, aspartic acid, and glutamic acid) in the samples are given in Table 1. Based on our experience, these are the most reliable amino acids in *Patella* spp. and *Thetystrombus latus* (Torres *et alii*, 2000; Ortiz *et alii*, 2015).

Fig. 5 - Field photographs of PS3. The top left capital letters indicate the sector of observation (see Fig. 1). The red arrow indicates a probable residual tidal notch (in photograph E) and an inner edge (in photograph F); the black arrows indicate lithophagid borings. Black horizontal lines with elevations in metres above the present sea level are indicated. ML: Mesozoic limestones; and br: continental breccias.

Fig. 6 - Field photographs of PS4. The top left capital letters indicate the sector of observation (see Fig. 1). For the photograph in sector E with sea caves, two features (photographs 1 and 2) have been reported: 1- a sea cave; 2- a small residual syn-wave-cut platform deposit (Unit IV) characterised by *Gastrochaenolites cor* (black arrow) with the original borer *Petricola lithophaga* (Retzius). Black horizontal lines with elevations in metres above the present sea level are indicated.

The numerical age could not be determined, as it would be necessary to have an age-calculation algorithm for *Patella* spp. shells from the Mediterranean realm.

Notwithstanding, the extensive use of AAR has allowed the establishment of a general aminostratigraphic framework of Pleistocene shorelines in the Mediterranean Basin (Table 1). Thus, the use of aminozones has permitted a more general application (Hearty *et alii*, 1986; Hearty, 1987; Torres *et alii* 2000). In this regard, relative dating can be established through aminostratigraphy: localities with similar D/L values are assumed to be synchronic.

In this regard, it should be considered that a same Aminozone is expressed by different value ranges of the D/L ratio, depending on the taxon considered; in this work we considered D/L value ranges of *Patella* sp. and *Thetystrombus latus* for the Aminozones (Torres *et alii*, 2000).

Thus, sampling sites MS1 (+ 15 m, PS3 and associated Unit III; see Figs. 1 and 9) and MS6 (+ 4.6 m, PS1 and associated Unit I; see Fig. 1) can be included within Aminozone E of Hearty *et alii* (1986) and Hearty (1987), which corresponds to MIS 5.5, as D/L values of *Patella*

Fig. 7 - Field photographs of PS5, PS6, and PS7 (reported in the top left) observed in sector F (Montagna Spaccata-Torre d'Alto Lido; see Fig. 1).

Fig. 8 - Field photographs (top) and a sketch (bottom) of a cliff in sector E (Uluzzo locality), showing the recognised palaeoshorelines and units. PS1, PS3, and PS4 of this figure are the same pictures in Fig. 3E (right photograph), 5E (top photograph), and 6E, respectively. The legend is valid also for Figure 9.

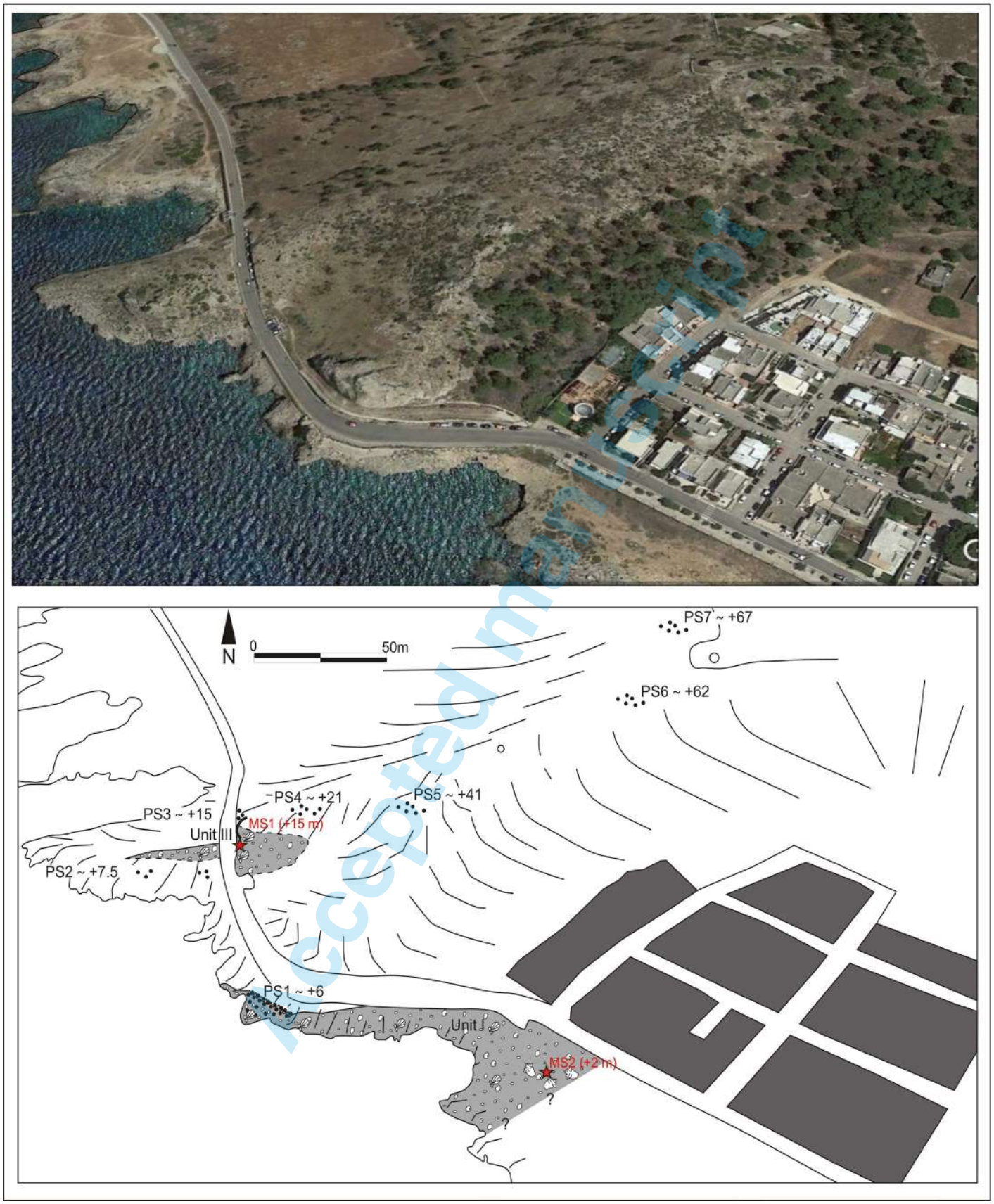

Fig. 9 - Google Earth image (top) and its sketch (down) of sector F ("Montagna Spaccata-Torre d'Alto Lido") showing the recognised palaeoshorelines and units. PS1, PS3, PS4, and PS5-PS7 of this figure are the same pictures in Figs. 3F, 5F, 6F, and 7, respectively. Note that PS1 indicate a palaeoshoreline at +6 m but, in sector F, the upper limit of the band of lithophagid borings can be observed at approximately +4.5 m. For the legend, see Fig. 8.

shells from these sites; similar (sensu Torres *et alii*, 2013 and references therein; see also caption of Table 1) than those of *Patella* shells from Cabo de Huertas, Mediterranean coast of Spain, whose deposits have been dated at 120±15 ka (Torres *et alii*, 2010).

Similarly, sampling site MS2 (+ 2 m, PS1 and associated Unit I; see Figs. 1 and 9) can be attributed to Aminozone E (MIS 5.5), as *Thetystrombus latus* shows D/L values similar to tyrrhenian deposits from Garrucha in Almería, Mediterranean coast of Spain (Torres *et alii*, 2000).

DISCUSSION

New AAR analyses, combined with the synchronous correlation technique, have been used to test different uplift rate scenarios to produce the best match between observed and expected palaeoshorelines.

We obtained the following two best fitting scenarios.

Scenario 1

This scenario is obtained using, as entered into the Terrace Calculator, the sea level curve of Siddall *et alii* (2003) until to 410 ky and Rohling *et alii* (2014) beyond 410 ky (Table 2, 1th and 2nd columns for sea level and age, respectively). Only for the 125 kyr BP highstand ~~did~~ we not refer to the sea level curve of Siddall *et alii* (2003), but to some specific studies conducted on the eustatic oscillations during that stage (Hearty *et alii*, 2007; O'Leary *et alii*, 2013; Dutton *et alii,* 2015 and references therein; Rohling *et alii*, 2019), from which it is shown that the most common value for the 125 ky BP highstand is + 6 m.

Scenario 1 implies an uplift rate of 0.15 mm/y until 130 ky BP (middle Pleistocene or interval MIS 15 - MIS 6; that is, 590 - 130 ky BP) and of 0.07 mm/y from 130 ky BP onwards (late Pleistocene or MIS 5 - onwards). This scenario takes into account literature data showing a similar uplift trend in the central-southern Apulian foreland (De Santis *et alii*, 2021; Ferranti & Oldow, 2006).

The uplift rate value of 0.07 mm/y is derived from a field interpretation of AAR results on Unit III and the associated PS3. Using the AAR results from sampling site MS1, PS3 and Unit III fall within aminozone E, that is, MIS 5.5. The well-preserved inner edge that characterises PS3 in sector F (Fig. 5F), the significant thickness of Unit III, and the elevation of +15 m a.p.s.l (which is ~~slightly higher than the maximum elevation of~~ MIS 5.5 deposits found along the Ionian coast between Taranto and Santa Maria di Leuca) allow us to hypothesise that PS3 and Unit III date back to the first peak of MIS 5.5; that is, 125 ky (10th column in Table 1).

From the AAR results from sampling sites MS2 and MS6, PS1 and Unit I also fall within aminozone E; that is, MIS ~~5~~. Nevertheless, given their minor elevation a.p.s.l., this allows us to assign PS1 and Unit I to a second peak of MIS 5.5; that is, 119 ky (10th column in Table 1), which has been recognised in other regions (Meschis *et alii*, 2020).

We conclude that the uplift rate value of 0.07 mm/y is derived by assigning an age of 125 ky (MIS 5.5) and a palaeo-sea level at +6 m (2nd column in Table 2) to PS3, which currently is at +15 m a.p.s.l, then with a vertical displacement of ca. 9 m in 125 ky.

The uplift rate value of 0.15 mm/y is derived from the iteration of uplift rates to find the scenario that offers the best match between expected and observed palaeoshorelines higher than PS3.

Scenario 2

Similar to scenario 1, scenario 2 is obtained using, as input into the terrace calculator, the sea level curve of Siddall *et alii* (2003) until to 410 ky and Rohling *et alii* (2014) after 410 ky (Table 2, 1st and 2nd columns for sea level and age, respectively), except for the 125 kyr BP highstand (+6 m), which is taken from more recent and specific literature (Hearty *et alii*, 2007; O'Leary *et alii*, 2013; Dutton *et alii,* 2015 and references therein; Rohling *et alii*, 2019).

Scenario 2 is derived from not attributing any of the palaeoshorelines falling into aminozone E to a specific ~~stage~~ but by iterating uplift rate values to find the best match between the mapped geomorphology and the expected sea level highstands, also respecting the constraint of MIS ~~5~~ for PS1, PS2, and PS3. The unique uplift rate that offers the best match between expected and

Table 1

Mean D/L values of isoleucine, aspartic acid and glutamic acid measured in *Patella* spp. and *Thetystrombus latus* shells from different localities. N: number of samples analysed. The eight samples from site MS1 are *Patella aspera* (Röding) and *P. caerulea* Linneo collected in sector F within Unit III associated with PS3 (see Figs. 5F and 9). The two samples from site MS2 are *Thetystrombus latus* collected in sector F within Unit I associated with PS1 (see Figs. 3F and 9). The three samples from site MS6 are *Patella* sp. and *Patella caerulea* Linneo collected in sector C within Unit I associated with PS1 (see Fig. 3C). For isoleucine, these D/L values were obtained with HPLC, while those from Cabo de Huertas were obtained by GC; the values obtained by HPLC required transformation in order to be compared with D/Lvalues measured by GC (Torres *et alii*, 2013).

sampling sites for AAR analyses	Associated palaeshoreline	Elevation of sampling site (m a. p.s.l.)	Taxa	N	D-allo/L-Ile	D/L Asp	D/L Glu	~~Age~~	Our age attribution (in Scenario 1)
MS1	PS3 (~+15 m)	+ 15 m	*Patella* spp	8	0.242±0.094	0.561±0.060	0.307±0.073	MIS 5.5	~~MIS 5.5 (~~125 ky~~)~~
MS6	PS1 (~ + 6 m)	+ 4.6 m	*Patella* spp	3	0.224±0.005	0.543±0.011	0.341±0.023	MIS 5.5	
MS2	PS1 (~ + 6 m)	+ 2 m	*T. latus*	2	0.496±0.129	0.619±0.049	0.483±0.093	MIS 5.5	

TABLE 2

Sea-level highstands (that is, expected palaeoshoreline elevations) and observed palaeoshorelines for scenarios 1 and 2. The expected palaeoshoreline elevations are derived by utilizing synchronous correlation using two input scenarios with sea level highstands from Siddall *et alii*, (2003) and Rohling *et alii* (2014) except for MIS 5.5 highstand (1st and 2nd columns for sea level and age, respectively), and: i) an uplift rate of 0.15 mm/y until 130 ky BP and of 0.07 mm/y starting from 130 ky BP; that is, scenario 1; and ii) a constant uplift rate of 0.12 mm/y; that is, scenario 2. Note that some expected palaeoshoreline elevations (560, 500, 410, 310, 285, and 200 ky BP) are lower than or equal to the next younger expected palaeoshoreline, suggesting that they may well be overprinted or re-occupied; that is, removed by erosion during rising sea level by the subsequent highstand. Thus, none of the observed palaeoshorelines were correlated with overprinted/re-occupied palaeoshorelines, with the exception of PS7 (560 ky BP in scenario 1; and 550 ky BP in scenario 2), which was considered partly overprinted. Note also that, given the uncertainty of ± 12 in sea level for the curve of Siddal *et alii* (2003), we consider acceptable gap of up to 10 m between an expected palaoshoreline (3rd column for scenario 1; and 4th column for scenario 2) and the observed palaeoshoreline we associate with it (5th, 6th, and 7th columns).

Ages of highstands (ky); from Siddal *et alii* (2003) and Rohling *et alii* (2014)	**Sea-level relative to today (mm); from Siddal *et alii* (2003) and Rohling *et alii* (2014). 125 kyr highstand from specific literature**	**Expected highstand-palaeoshoreline elevations (m); scenario 1**	**Expected highstand-palaeoshoreline elevations (m); scenario 2**	**DTM/field observed palaeoshoreline elevations (m) and our association with expected palaeoshorelines; scenario 1**	**DTM/field observed palaeoshoreline elevations (m) and our association with expected palaeoshorelines; scenario 2**	**Comments on our association between expected and observed palaeoshorelines**	**MIS**
0	0	0	0	0			
30	-80000	-78	-76			submerged	
50	-60000	-56	-54			submerged	
76.5	-30000	-24	-21			submerged	
100	-25000	-18	-13			submerged	
115	-21000	-13	-7			submerged	
119	-5000	4	9	6/7.5	6/7.5	PS1 +PS2	5.5
125	6000	15	21	15	15	PS3	5.5
175	-30000	-14	-9			submerged	6.5
200	-5000	15	19			overprinted/re-occupied by 125 ky BP highstand	7.1
217	-30000	-8	-4			submerged	7.3
240	-5000	21	24	21	21	PS4	7.5
285	-30000	3	4			overprinted	8.5
310	-22000	10	15			overprinted	9.1
340	5000	46	46	41	41	PS5	9.3
410	-5000	46	44			overprinted/re-occupied by 340 ky BP highstand	11
478	0	62	57	62	62	PS6	13.1
525	20000	89	83			Higher than the maximum elevation of the study area in both scenarios 1 and 2	13.3
550	10000	82	76		67	PS7 in scenario 2 (partly overprinted). Higher than the maximum elevation of the study area in scenario 1	15.1 (?)
560	3000	77	70	67		PS7 in scenario 1(partly overprinted)	15.1 (?)
590	20000	98	91			Higher than the maximum elevation of the study area in both scenarios 1 and 2	15.3

observed palaeoshorelines is 0.12 mm/y for the entire time span considered: 590 ky onwards (that is, middle-late Pleistocene or MIS 15 onwards).

Comparison between field/DTM-based and expected palaeoshorelines

In this section, we show how our GIS and field-based results are correlated with the suggested uplift models.

The expected sea-level highstands (that is, expected palaeoshoreline elevations) generated by our synchronous correlation method (via the Terrace Calculator spreadsheet) are listed in the 3rd and 4th columns (for scenarios 1 and 2, respectively) in Table 2.

We have associated the expected palaeoshorelines with the observed palaeoshorelines as indicated in the 5th, 6th, and 7th columns in Table 2 and in Figures 10 (for scenario 1) and 11 (for scenario 2).

Given the uncertainty of ± 12 in sea level for the curve of Siddal *et alii* (2003), we consider acceptable a gap of up to 10 m between an expected and the observed palaeoshoreline we associate with it (compare the 3rd and 4th columns in Table 2 with the 5th and 6th columns, respectively).

Ultimately, the palaeoshorelines recognised in the field in this study refer to the following highstands: 119 (MIS 5.5, second peak; Hearty *et alii*, 2007; Rohling *et alii*, 2008; Kopp *et alii*, 2009, 2013; O'Leary *et alii*, 2013; Dutton *et alii,* 2015 and references therein; Dusterhus et al, 2016), 125 (MIS 5.5), 240 (MIS 7.5), 340 (MIS 9.3), and 478 (MIS 13.1) for both scenarios 1 and 2. The two scenarios diverge only for the oldest palaeoshoreline: 560 ky BP (MIS 15.3) in scenario 1 and 550 ky BP (MIS 15.1) in scenario 2. These sea level highstands have been recognised within the Mediterranean realm by previous investigations (e.g., Roberts *et alii*, 2009, 2013; Meschis *et alii*, 2018, 2020; Robertson *et alii*, 2019).

For both scenarios 1 and 2, some expected sea level highstand elevations (560, 550, 410, 310, 285, and 200 ky BP; 3rd and 4th columns in Table 2) are lower or (near) equal to the next younger expected palaeoshoreline, suggesting that they may well be overprinted or re-occupied; that is, removed by erosion during rising sea level of the subsequent highstand. Thus, none of the observed palaeoshorelines have been correlated with overprinted or re-occupied palaeoshorelines. The only exception is represented by PS7 (560 ky in scenario 1 and 550 ky in scenario 2), which was partially preserved despite being overprinted by two subsequent highstands dating back to 550 and 525 kyr BP in scenario 1 or by a single subsequent highstand dating back to 525 in scenario 2. In scenario 2, PS7 could be attributed to both 550 and 560 kyr highstands because in both cases, the difference between the expected and observed palaeoshoreline is less than 10 m. We preferred to attribute it to the 550 kyr highstand (Table 2, 6th and 7th columns) because, based on this scenario, the 550 kyr highstand would have undergone only one overprinting by the 525 kyr highstand and therefore, it is the one most likely to have been preserved until today, at least in part.

In addition, the synchronous correlation technique also highlights the presence of several submerged palaeoshorelines at the present day, many of which are probably completely overprinted.

Figures 10 and 11 show, for two of the four topographic profiles extracted from the DTM, the elevations of observed (coloured arrows) against expected (horizontal lines) palaeoshoreline elevations according to scenario 1 (Fig. 10) and scenario 2 (Fig. 11). In these figures, the association between expected and observed palaeoshoreline elevations is represented, using the same-coloured horizontal lines to represent the expected highstand elevations and arrows to represent the corresponding observed palaeoshorelines.

For both scenarios, field-measured against expected palaeoshoreline elevations show an R^2 value of 0.99 (Fig. 12a, b for scenarios 1 and 2, respectively). This value confirms that the fits between expected and observed palaeoshorelines are good, giving confidence to the uplift rates.

Overview of the terrace phases and vertical movements of the Apulian foreland in the middle-late Pleistocene

The Apulian foreland represents one of the uncommon cases of a foreland shared by two opposite-verging chains: the SW-verging Albanides-Hellenides and NE-verging southern Apennines. The deformation occurring within this type of foreland is uncommon and poorly understood.

To date, the Apulian foreland has been characterised by a scarcity of reliable chronological data concerning the marine terraces and therefore the associated vertical crustal displacement rates in the middle Pleistocene (Cerrone *et alii*, in press). To date, most uplift rates of the Apulian foreland have only been estimated for the late Pleistocene by using the elevation of the marine terrace related to the last interglacial period (MIS 5.5) (Hearty & Dai Pra, 1992; Belluomini *et alii*, 2002; Mastronuzzi *et alii*, 2007).

The new chronological constraints and results of the synchronous correlation presented in this work are, along with results recently published in De Santis *et alii* (2021), the first obtained for the middle Pleistocene along the entire coastal stretch of the Apulian foreland from Trani to Taranto (central southern Adriatic coast and Ionian coast between Otranto and Taranto).

In both scenarios, PS1 and PS2 are referred to the highstand at 119 ky BP; the presence of sectors in the study area where scattered lithophagid borings in the Mesozoic limestone are interposed between PS1 and PS2 seems to confirm this reconstruction, along with the uncertainties in the stratigraphic relationship between Units I and II. Most likely, PS1 and PS2, as well as Units I and II, are to be referred to sea level stillstands within the highstand at 119 ky BP.

Furthermore, in both scenarios, the expected highstands at 200 and 125 ky BP (MIS 7.1 and 5.5, respectively) are very close in elevation or equal (3rd and 4th columns in Table 2), while we have only recognised PS3 at +15 m a.p.sl. in the field, attributed to 125 ky BP (MIS 5.5) (5th, 6th and 7th columns in Table 2). We cannot rule out that the older highstand at 200 ky BP (MIS 7.1) was re-occupied by the younger PS3; consequently, PS3, as can be observed today, could contain features inherited in some cases from the MIS 7.1 highstand, in some cases from the MIS 5.5 highstand, and in some cases from both the MIS 7.1 and 5.5 highstands. Similarly, this can be applied to the expected highstands at 410 and 340 ky BP (MIS 11 and 9.3, respectively); thus, the observed PS5 at +41 m a.p.sl., attributed to 340 ky BP (MIS 9.3) (5th, 6th and 7th columns

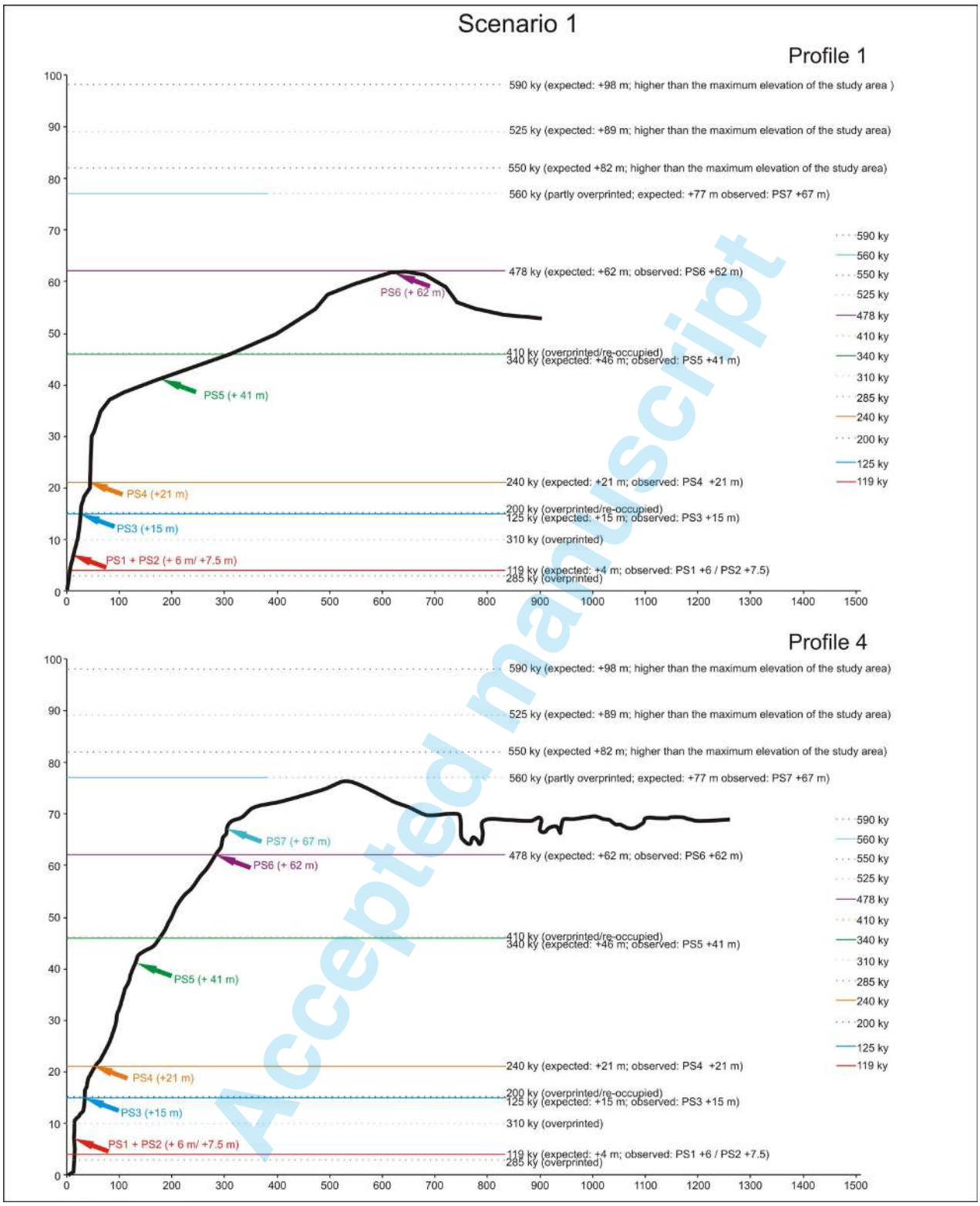

Fig. 10 - Scenario 1. Elevations of observed palaeoshorelines (coloured arrows) against expected palaeoshorelines (horizontal, coloured lines) using the synchronous correlation (via Terrace Calculator) for topographic profiles 1 (up) and 4 (down). The scenario of expected palaeoshorelines was obtained with an uplift rate of 0.15 mm/y until 130 ky and of 0.07 mm/y from 130 ky onwards. Each horizontal line marked with a certain colour represents an expected palaeoshoreline elevation; the arrow of the same colour represents the corresponding observed palaeoshoreline. Note that some expected palaeoshoreline elevations (560, 550, 410, 310, 285 and 200 ky BP) are lower than or equal to the next younger expected palaeoshoreline, suggesting that they may well be overprinted or re-occupied (dashed horizontal lines, which also indicate expected palaeoshorelines higher than the maximum elevation of the study area). Thus, none of the observed palaeoshorelines have been correlated with overprinted or re-occupied palaeoshorelines. The only exception is represented by PS7, attributed in this scenario to 560 ky. The elevations in m. a. p.s.l. of the horizontal lines and arrows are the same as those in the 3rd and 4th columns in Table 2, respectively. Since both the expected and observed palaeoshorelines are at the same heights for the entire study area, they have been reported only on two topographic profiles.

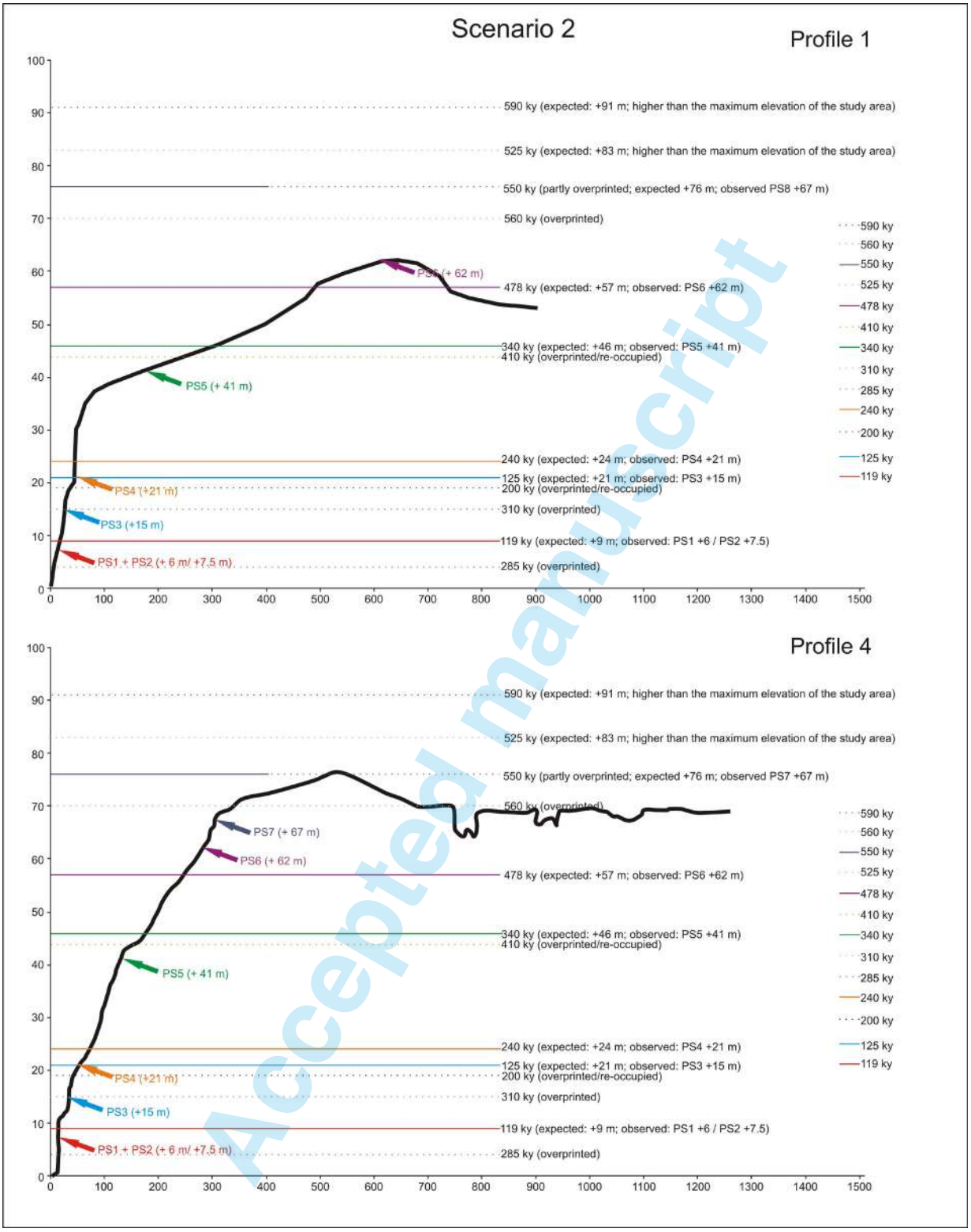

Fig. 11 - Scenario 2. Elevations of observed palaeoshorelines (coloured arrows) against expected palaeoshorelines (horizontal, coloured lines) using the synchronous correlation (via Terrace Calculator) for topographic profiles 1 (up) and 4 (down). The scenario of expected palaeoshorelines was obtained with a constant uplift rate of 0.12 mm/y. Each horizontal line marked with a certain colour represents an expected palaeoshoreline elevation; the arrow of the same colour represents the corresponding observed palaeoshoreline. Note that some expected palaeoshoreline elevations (560, 550, 410, 310, 285 and 200 ky BP) are lower than or equal to the next younger expected palaeoshoreline, suggesting that they may well be overprinted or re-occupied (dashed horizontal lines, which also indicate expected palaeoshorelines higher than the maximum elevation of the study area). Thus, none of the observed palaeoshorelines have been correlated with overprinted or re-occupied palaeoshorelines. The only exception is represented by PS7, attributed in this scenario to 550 ky. The elevations in m. a. p.s.l. of the horizontal lines and arrows are the same as those in the 3rd and 4th columns in Table 3, respectively. Since both the expected and observed palaeoshorelines are at the same heights for the entire study area, they have been reported only on two topographic profiles.

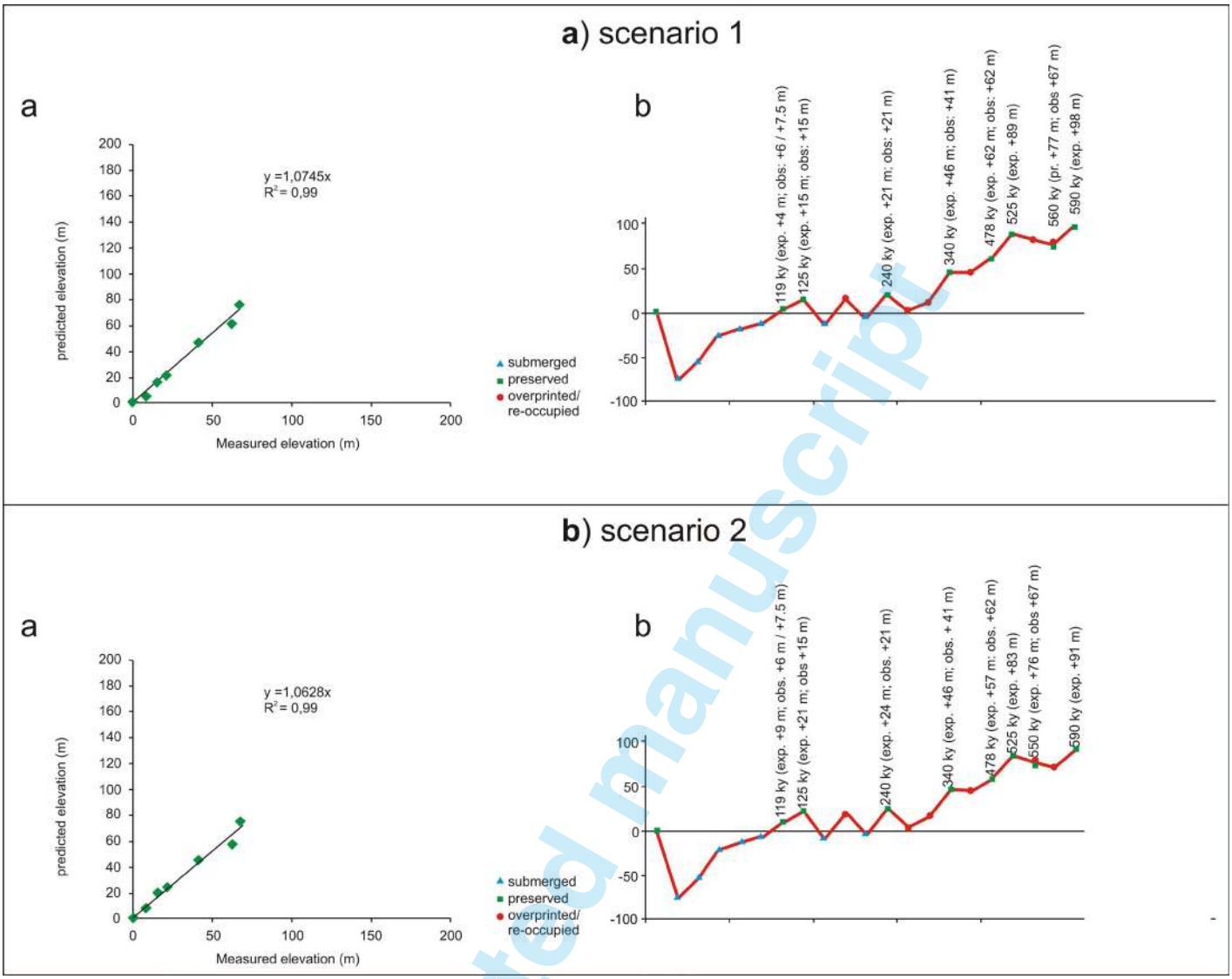

Fig. 12 - Scenario 1 (a) and scenario 2 (b). a) Graph showing linear regressions between observed and expected palaeoshoreline elevations. Good fit is quantified by R^2 values that are ≥ 0.99. b) Expected palaeoshoreline elevations; graph shows the palaeoshorelines submerged and those overprinted (red squares). Both graphs are valid for all topographic profiles, as the palaeoshorelines observed in several profiles are always at the same elevation (m.a.p.s.l.).

in Table 2), could be the result of a re-occupation between the highstands at 410 and 340 ky BP.

Although up to now, data on vertical movements have referred to the middle Pleistocene and based on reliable chronological constraints are almost completely missing for the Salento sector, some literature data concerning the vertical movements of the Apulian foreland in the middle-late Pleistocene seem to support scenario 1; that is, a decrease in uplift rate over time. For example, Ferranti & Oldow (2006) reported that much of the uplift in Gargano occurred between the middle-late Miocene and early Pliocene at ~0.06 mm/y, while uplift of Murge occurred steadily at ~0.5 mm/y from 1.3 Ma to 130 ky; during the late Pleistocene, coherent behaviour of the two blocks can be inferred, with a common uplift rate decreasing to ~0.20 mm/y. In this framework, this study could insert the new element of a similar uplift trend for the Salento sector, albeit with lower uplift values compared with those in Gargano and Murge.

A decreasing trend in the middle-late Pleistocene uplift rate also appears from the data on the marine terraces of the Ionian coast west of Taranto (De Santis *et alii*, 2018) and of the area around the city of Bari (De Santis *et alii*, 2021)

Moreover, for the eastern coast of the Salento Peninsula from Otranto to Santa Maria di Leuca, a change in the uplift rate is hypothesised, even if with different times than our study area. According to Mastronuzzi *et alii* (2007), a marine terrace staircase most likely formed during a phase of uplift that occurred in the early Pleistocene and/or in the early middle Pleistocene, and the coastal stretch became stable after the end of the middle Pleistocene (MIS 9).

The uplift evidenced by sequences of marine terraces in the Apulian foreland seems to be related to the more generalised uplift that characterised the chain, foredeep and Apulian foreland since the middle Pleistocene; the so-called Ionian bulge (Ferranti *et alii*, 2006). This large-scale topographic bulge, recorded by uplift and deformation of

the MIS 5.5 terrace, has maximum topographic evidence in Calabria and NE Sicily and progressively vanishes towards the Apulia region to the north and the Hyblean Plateau to the south (Westaway, 1993; Ferranti *et alii*, 2006; Faccenna *et alii*, 2011).

The cause of the Ionian bulge is currently a matter of debate; some of the hypotheses are as follows:

1) Lithospheric rebound in response to the breakup of the underlying slab (e.g., Cinque *et alii*, 1993; Westaway, 1993).
2) Mantle upwelling occurring under the Apennine belt could be responsible for the observed uplift and crustal extension (D'Agostino *et alii*, 2001; Lavecchia *et alii*, 2003).
3) Dynamic mantle upwelling, in turn related to the formation and enlargement of slab windows below the southern-central Apennines starting in the early Pleistocene (Faccenna *et alii*, 2007, 2014).

Scenario 1, without adding anything to the debate on the cause of the Ionian bulge, would confirm that, whatever the mechanism that triggered the bulge, it was decreasing, at least in the Apulian foreland.

However, the weaknesses of scenario 1 are that it does not explain the reason for the uplift slowdown, which also appears as an unexpected phenomenon in a stable foreland such as the Apulian foreland. Furthermore, in the future, to support scenario 1, it will be necessary to establish whether the other previous studies carried out thus far, which seem to show the previously mentioned slowdown in the uplift rate, can also be confirmed by taking into account the overprinting of palaeoshorelines; that is, these results should be evaluated with the synchronous correlation approach.

Scenario 2 is simpler; it does not require the explanation of a change in uplift rate, and it is well suited to a geodynamically stable foreland such as the Apulian foreland.

In addition, for both scenarios, there is the difference between the model and reality to consider. For example, for scenario 1, it could be very likely that the decrease in the uplift rate was much more gradual over time and not instantaneous, as in our model.

Regardless of the scenarios developed on the uplift rates, a fundamental characteristic of the palaeoshorelines we recognised is that they can be observed at the same elevation a.p.s.l. for the entire study area; this feature indicates that there are no active faults that have displaced the coastal sector of the study area into blocks with differential uplift and suggests that, at least in the middle and late Pleistocene, this sector of the Salento Peninsula has risen uniformly (regardless of how fast it raised, it raised all together).

Nevertheless, the chronological attribution and current elevation of PS3 and Unit III (125 ky BP and +15 m a.p.s.l., respectively) suggest that they could form the palaeoshoreline and deposit of MIS 5.5 found at an elevation which is one of the highest among those reported in previous studies between Taranto and Santa Maria di Leuca (Hearty & Dai Pra, 1992; Belluomini *et alii*, 2002), which, however, had never considered the coastal stretch of this study. One of the possible explanations could be a tectonic uplift of this sector of the Salento Peninsula greater than that of adjacent coastal stretches, probably due to the recent activity of normal faults. Indeed, south of our study area, some normal faults where the footwall N-NE block moved upward relative to the S-SW hanging wall block have been reported in the official geological cartography (Largaiolli *et alii*, 1969), in the Neotectonic map of Itay (Ambrosetti *et alii*, 1987), and in a study on the tectonic set-up of the southern Apulian foreland (Tozzi, 1993).

Another possible conciliation between the elevation of the 125 ky palaeshoreline reported in this study and the elevations of the MIS 5.5 deposits documented so far in the Ionian coast between Taranto and Santa Maria di Leuca is that the latter are the lowest deposits of MIS 5.5, that is, those related to the second peak of MIS 5.5 (119 ky BP).

For future works, we stress that more investigations are needed to confirm both the elevation of +15 m of the palaeoshoreline at 125 ky BP for this area and the possible causes for this elevation.

Comparison with other Mediterranean sites

Palaeoshorelines dating back to the middle-late Pleistocene recognised in other perimediterranean areas, in which there are wide palaeohoreline staircases, in most cases, have a different spatial and temporal organisation, linked to different geodynamic contexts. Here are some examples of emerged palaeoshorelines, with the ages to which they have been attributed, from the lowest to the highest:

1) Area of Vibo Valentia (Tyrrhenian coast of the Calabria region, southern Italy): 11 palaeoshorelines attributed to 50, 76.5, 100, 125, 178, 200, 217, 240, 285, 310, and 340 ky BP (Roberts *et alii*, 2013).
2) Area of Capo D'Orlando (Tyrrhenian coast of the Sicilia region, southern Italy: 10 palaeoshorelines attributed to 76.5, 100, 125, 178, 200, 217, 240, 285, 310, and 340 ky BP (Meschis *et alii*, 2018).
3) SE Sicily, along the Ionian coastal sector: 9 palaeoshorelines attributed to 119, 125, 200, 240, 310, 340, 410, 478, and 525 ky BP (Meschis *et alii*, 2020).
4) SW Sicily: 11 palaeoshorelines attributed to 82, 103, 124, 167, 197, 215, 236, 287, 313, 331, and 406 ky BP (Ferranti *et alii*, 2021).
5) Ionian coast of southern Italy: 18 palaeoshorelines attributed to 5-10, 30-35, 45-50, 55-65, 70-80, 80-85, 85-95, 10-105, 115-125, 165-180, 185-200, 225-240, 280-295, 305-315, 320-335, 390-410, 480-500, and 570-590 ky BP (Caputo *et alii*, 2010).
6) South Crete (Greece): 9 palaeoshorelines attributed to 76.5, 100, 125, 175, 200, 240, 310, 340, and 410 ky BP (Robertson *et alii*, 2019).
7) Gulf of Corinth (Greece): 8 palaeoshorelines attributed to 76, (possibly) 100, 125, 175, 200, 216, 240, and 340 ky BP (Roberts *et alii*, 2009).

All areas listed above, characterised by the extensive presence of palaeoshorelines dating back to the middle-late Pleistocene, are characterised by uplift rates higher than those of the Apulian foreland presented in this study (uplift rates between 0.4 and 1.75 mm/y in the area of Vibo Valentia, between 0.4 and 0.89 mm/y in the area of Capo D'Orlando, between 0.16 and 0.41 mm/y in SE Sicily,

between 0.46 and 0.82 mm/y in SW Sicily, between 0.2 and 2 mm/y along the Ionian coast of southern Italy, between 0.24 and 0.89 mm/y in south Creete, and between 0.15 and 0.51 mm/y in the Gulf of Corinth).

There is therefore a fundamental difference between the palaeoshorelines of the Apulian foreland and the others listed above: generally, in the Apulian foreland, a smaller number of highstands left a trace in the form of a palaeshoreline. Due to the low uplift rates, the palaeoshorelines have undergone overprinting or re-occupation phenomena, or are now submerged: the synchronous correlation technique highlights this situation- Extensive overprinting and re-occupation, symptomatic of low uplift rates, have also been observed on the Cotentin Peninsula (France; Pedoja *et alii*, 2018).

The synchronous correlation technique, applied for the first time to the Apulian foreland, modifies the previously applied technique, known as "sequential correlation" (e.g., Roberts *et alii.*, 2013; Robertson *et alii.*, 2019), where, starting from a single dated palaeoshoreline, it is assumed that the next higher and older palaeoshoreline belongs to the next older sea level highstand. It is therefore probable that this classic methodological approach, if accompanied by the absence of reliable datings, is risky in all cases of fairly stable territories or with weak and constant vertical movements, such as that in the Apulian foreland, because it does not highlight cases of overprinting, which instead are highly probable in these geodynamic contexts.

Other possible age attribution for PS1 and PS2

For this work we used well-known and world-recognised sea level curves, which report MIS 5.3 and 5.1 highstands too low to have emerged today in low uplift areas such as the Apulian foreland; for this reason, the paleoshorelines of MIS 5.3 and 5.1 did not emerge in our modelling.

In contrast, a growing number of works have by now evidenced much higher sea levels, close to the present sea level, for MIS 5.3 and 5.1 in several regions of the world, challenging the notion of a sea level 20 to 30 m lower than in the present time. Medina-Elizade (2013) provided a review of the sea level benchmarks from several coral reefs in different regions of the world, showing the occurrence of sea levels close to the present during both MIS 5.3 and MIS 5.1. Similarly, Vicens *et alii* (2012) and Zazo *et alii* (2013) suggested similar paleo-sea levels for MIS 5.5 and either MIS 5.3 or MIS 5.1 for the Mediterranean Sea based on data from Mallorca Island in the Balearic archipelago. Finally, Marra *et alii* (2016, 2019, 2020) provided evidence for anomalous sea levels during MIS 5.3 and MIS 5.1 both in the tectonically active and in the stable sectors of the Tyrrhenian Sea coast of Latium (central Italy): paleo sea levels of 0 m and -6 m a.s.l. were assessed for MIS 5.3 and MIS 5.1, respectively, in the coast comprised between the Tiber mouth and Anzio promontory. Similar high paleo-sea levels for MIS 5.3 and 5.1 have been also proposed by Marra *et alii* (2020) based on sea-level markers occurring at several coastal caves in the supposedly stable (Ferranti *et alii*, 2006; Antonioli *et alii*, 2015) sector comprised between the Circeo promontory and the Gaeta gulf.

Indeed, using the highstand elevations proposed by Marra *et alii* (2020) for MIS 5.3 and 5.1 in our modelling via Terrace Calculator (both for scenarios 1 and 2), their resulting present elevations are very close to our observed shorelines PS2 and PS1, respectively.

This result, however, would conflict with: 1) the AAR analysis conducted on *Thetystrombus latus* taken from the sampling site MS2 (+ 2 m, PS1 and associated Unit I; see Figs. 1 and 9 and Tab. 1) which can be attributed to Aminozone E (MIS 5.5); 2) the field evidence that, in sampling site MS2, *Thetystrombus latus* specimens are embedded into a proximal pebbly beach deposit (Unit I), laterally passing to sandy-calcarenite deposits; this proximal deposit appears to be genetically associated with PS1, as constitutes the syn-wave-cut platform deposit coeval with PS1.

However, it should be considered the time-averaging. According to Torres *et alii* (2013), as a result of time-averaging and post-depositional processes, it may be difficult to identify substages. In this regard, as in many other sedimentary environments, beach deposits are time-averaged, and different factors can affect the scale of temporal mixing, including some intrinsic to particular species and others related to depositional environments. Temporal mixing depends on the skeletal durability of shells (Kowalewski, 1997) since durable shells can survive multiple reworking events and long residence times and may undergo temporal mixing on a scale of hundreds to thousands of years (Behrensmeyer, 1991; Flessa *et alii*, 1993). Other factors which can affect the AAR results are those related to depositional environments, which include sedimentation rate, bioturbation, and taphonomical processes such as chemical dissolution, mechanical fragmentation and bioerosion (Davies *et alii*, 1989; Meldahl *et alii*, 1997; Kidwell, 1998; Carroll *et alii*, 2003; Kidwell *et alii*, 2005).

In light of these factors, today we cannot completely rule out the hypothesis that PS1 and PS2 are not referable to the second peak of MIS 5.5, but are to be referred to MIS 5.1 and 5.3 highstands, respectively. However, further investigations and more detailed dating are needed to test this alternative hypothesis.

CONCLUSIONS

For the first time in Apulian foreland (western coast of the Salento Peninsula, southern Italy) and the second time in Italy, the synchronous correlation technique was applied to an understudied sequence of raised palaeoshorelines to refine the knowledge about terrace phases and uplift history in the middle-late Pleistocene. This technique has been used together amino acid racemization (AAR) analyses of *Patella* spp. and *Thetystrombus latus* shells, which are the most widespread taxa in the study area and suitable for chronological analysis. These combined methodologies provide the first chronological attribution, at a MIS scale, for middle-late Pleistocene palaeoshorelines and quantitative assessment of vertical crustal movements in this sector of the Apulian foreland, which, to date, has been characterised by a scarcity of reliable chronological data.

By applying the synchronous correlation technique driven by new AAR analyses, we find the best match between field-based observed palaeoshorelines and "expected" sea level highstand elevations.

Our results show that two uplift rate scenarios could explain the mapped geomorphology: (i) scenario 1

suggests an uplift rate of 0.15 mm/y until 130 ky (middle Pleistocene, interval MIS 15 - MIS 6; that is, 590 - 130 ky BP) and of 0.07 mm/y from 130 ky BP to the present; on the other hand, (ii) scenario 2 suggests a constant uplift rate of 0.12 mm/y over time in the middle-late Pleistocene.

The palaeoshorelines recognised in this study, from the lower to the higher elevation a.p.s.l., are the following: PS1 and PS2: 119 ky BP (MIS 5.5 second peak), PS3: 125 ky BP (MIS 5.5), PS4: 240 ky BP (MIS 7.5), PS5: 340 ky BP (MIS 9.3), and PS6: 478 ky BP (MIS 13.1) for both scenarios 1 and 2. The two scenarios only differ in the oldest and highest palaeoshoreline, PS7: 560 ky BP (MIS 15.3) in scenario 1 and 550 ky BP (MIS 15.1) in scenario 2.

We show that fewer palaeoshorelines are preserved than in regions where higher uplift rates have been inferred, suggesting a more prominent effect of the "overprinting" or re-occupation of younger sea level highstands over the older sea level highstands. Finally, in the light of a growing number of works which have by now evidenced much higher sea levels, close to the present sea level, for MIS 5.3 and 5.1 in several regions of the world, today we cannot completely rule out the hypothesis that PS1 and PS2 are not referable to the second peak of MIS 5.5, but are to be referred to MIS 5.1 and 5.3 highstands, respectively. For this latter, we stress that future detailed investigations are needed.

Acknowledgements

We wish to thank all the staff at the Polo Scientifico e Tecnologico Magna Grecia (Taranto) for the topographic instruments. We kindly thank Fabrizio Marra and Ciro Cerrone for their constructive reviews, allowing to improve this manuscript. Finally, last but not least, a special thanks goes to prof. Giovanni Scicchitano, for his continuous and fruitful contribution during all phases of the research and drafting of the manuscript.

REFERENCES

Ambrosetti P., Bosi C., Carraro F., Ciaranfi N., Panizza M., Papani G., Vezzani L. & Zanferrari A. (1987) - *Neotectonic Map of Italy: Scale 1:500000*. Consiglio Nazionale delle Ricerche, Progetto Finalizzato Geodinamica, Sottoprogetto Neotettonica. Litografia Artistica Cartografica, Florence (Italy).

Amorosi A., Antonioli F., Bertini A., Marabini, S., Mastronuzzi G., Montagna P., Negri, A., Rossi V., Scarponi D., Taviani M., Angeletti L., PivaA. & Vai G.B. (2014) - *The Middle-Upper Pleistocene Fronte Section (Taranto, Italy): An exceptionally preserved marine record of the Last Interglacial*. Global and Planetary Change, **119**, 23-38.

Antonioli F, Ferranti L, Stocchi P., Deiana G., Lo Presti V., Furlani S., Marino C., Orru P., Scicchitano G., Trainito E., Anzidei M., Bonamini M., Sansò P. & Mastronuzzi G. (2018) - *Morphometry and elevation of the last interglacial tidal notches in tectonically stable coasts of the Mediterranean Sea*. Earth-Science Reviews, **185**, 600-623.

Antonioli F., Lo Presti V., Rovere A., Ferranti L., Anzidei M., Furlani S., Mastronuzzi, G., Orru P.E., Scicchitano G., Sannino G., Spampinato C.R., Pagliarulo R., Deiana G., de Sabata E., Sanso P., Vacchi M. & Vecchio A. (2015). *Tidal notches in Mediterranean Sea: a comprehensive analysis*. Quaternary Science Reviews, **119**, 66-84.

Azzaroli A. (1968) - *Calcarenite di Gravina. Studi illustrativi della Carta Geologica d'Italia* - Servizio Geologico d'Italia, Formazioni Geologiche, Fasc. **1**, 183-187.

Azzaroli A., Perno U. & Radina B. (1968) - *Note illustrative del Foglio 188 "Gravina di Puglia" della Carta Geologica d'Italia alla scala 1:100.000*. Servizio Geologico d'Italia, Roma.

Belluomini G., Caldara M., Casini C., Cerasoli M., Manfra L., Mastronuzzi G., Palmentola G., Sansò P., Tuccimei P. & Vesica P.L. (2002) - *The age of Late Pleistocene shorelines and tectonic activity of Taranto area, Southern Italy*. Quaternary Science Reviews, **21**, 525-547.

Behrensmeyer A.K. (1991) - *Terrestrial vertebrate accumulations*. In: Allison P., Briggs E.G. (Eds.), *Taphonomy: Releasing the Data Locked in the Fossil Record*. Plenum, New York, pp. 291-335.

Benjamin J., Rovere A., Fontana A., Furlani S., Vacchi M., Inglis R.H., Galili E., Antonioli F., Sivan D., Miko S. & Mourtzas N. (2017) - *Late Quaternary sea-level changes and early human societies in the central and eastern Mediterranean Basin: An interdisciplinary review*. Quaternary International, **449**, 29-57

Bloom A.L. (1980) - *Late Quaternary sea level change on South Pacific coasts: a study in tectonic diversity*. In Morner N.A. (ed), *Earth rheology, isostasy and eustacy*: Proceedings of Earth Rheology and Late Cenozoic Isostatic Movements Conference, 1977, Stockholm, 505-516.

Boenzi F., Caldara M. & Pennetta L. (1986) - *La trasgressione tirreniana nei dintorni di Castellaneta (Taranto)*. Geologia Applicata ed Idrogeologia, **20**(1), 163-175.

Boenzi F., Caldara M. & Pennetta L. (2010) - *L'ambiente fisico e la distribuzione dei vini nella regione pugliese*. In: *Storia regionale della vite e del vino in Italia: le Puglie. La Daunia, la Terra di Bari, la Terra d'Otranto*, a cura di Calò A. & Bertoldi Le Noci L., 17-31, Edizioni Pugliesi s.r.l. Martina Franca, ISBN 9788883481642.

Boscato A. & Crezzini J. (2012) - *Middle-Upper Palaeolithic transition in Southern Italy: Uluzzian macromammals from Grotta del Cavallo (Apulia)*. Quaternary International, **252**, 90-98.

Brückner H. (1980) - *Marine Terrassen in Süditalien. Eine quartärmorphologische Studie über das Küstentiefland von Metapont*. Düsseldorfer Geographische Schriften, **14**, 235 pp., Düsseldorf (PhD thesis).

Caldara M., Iannone A., Lopez R., Simone O., De Santis V., Torres T. & Ortiz J.E. (2013) - *New data on the Pleistocene of Trani (Adriatic coast, southern Italy)*. Italian Journal of Geosciences, **132**(2), 239-253.

Caldara M., Mastronuzzi G., Palmentola G., Sansò P., Tuccimei P. & Vesica P.L. (2003) - *Reply to the comment by P.J. Hearty and G. Dai Pra*. Quaternary Science Reviews, **22**(4-6), 2369-2371.

Caputo R., Bianca M. & D'Onofrio R. (2010) - *Ionian marine terraces of southern Italy: Insights into the Quaternary tectonic evolution of the area*. Tectonics, **29**(4), TC4005.

Carroll M., Kowalewski M., Simões M.G. & Goodfriend G.A. (2003) - *Quantitative estimates of time-averaging in terebratulid brachiopod shell accumulations from a modern tropical shelf*. Paleobiology, **29**, 381-402.

Cerrone C., Vacchi M., Fontana A. & Rovere A. (in press) - *Last Interglacial sea-level proxies in the Western Mediterranean*, Earth Syst. Sci. Data Discuss. [preprint], https://doi.org/10.5194/essd-2021-49, in review, 2021.

Ciaranfi N., Pieri P. & Ricchetti G. (1992) - *Note alla carta geologica delle Murge e del Salento (Puglia centro-meridionale)*. Memorie della Società Geologica Italiana, **41**(1988), 449-460.

Cinque A., Patacca E., Scandone P. & Tozzi M. (1993) - *Quaternary kinematic evolution of the southern Apennines. Relationship between surface geological features and deep lithospheric structures*. Annali di Geofisica, **36**(2), 249-260.

D'Agostino N., Jackson J.A., Dramis F. & Funiciello R. (2001) - *Interactions between mantle upwelling, drainage evolution and active normal faulting: an example from the central Apennines (Italy)*. Geophysical Journal International, **147**, 475-479.

Dai Pra G. & Stearns C.E. (1977) – Sul Tirreniano di Taranto. Datazioni su coralli con il metodo del Th^{230}/U^{234}. Geologica Romana, **16**, 231-242.

D'Argenio B. (1974) - *Le piattaforme carbonatiche periadriatiche. Una rassegna di problemi nel quadro geodinamico mesozoico dell'area mediterranea*. Memorie della Società Geologica Italiana, **13**, 137-160.

Davies D.J., Powell E.N. & Stanton R.J. (1989) - *Relative rates of shell dissolution and net sediment accumulation – a commentary: can shell beds form by the gradual accumulation of biogenic debris on the sea floor?* Lethaia, **27**, 207-212.

De Giosa F., Scardino G., Vacchi, M., Piscitelli A., Milella M., Ciccolella A. & Mastronuzzi, G. (2019) - Geomorphological signature of late Pleistocene sea level oscillations in Torre Guaceto marine protected area (Adriatic Sea, SE Italy). Water, **11**(11), 2409.

Demarchi B., Collins M.J., Tomiak P.J., Davies B.J. & Penkman K.E.H. (2013a) - *Intra-crystalline protein diagenesis (IcPD) in Patella vulgata. Part II: Breakdown and temperature sensitivity.* Quaternary Geochronology, **16**(100), 158-172.

Demarchi B., Rogers K., Fa D.A., Finlayson C.J., Milner N. & Penkman K.E.H. (2013b) - *Intra-crystalline protein diagenesis (IcPD) in Patella vulgata. Part I: Isolation and testing of the closed system*. Quaternary Geochronology, **16**, 144-157.

Demarchi B., Williams M.G., Milner N., Russell N., Bailey G.N. & Penkman K.E.H. (2011) - *Amino acid racemization dating of marine shells: a mound of possibilities*. Quaternary International, **239**, 114-124

De Santis V. & Caldara M. (2016) - *Evolution of an incised valley system in the southern Adriatic Sea (Apulian margin): an onshore–offshore correlation*. Geological Journal, **51**(2), 263-284.

De Santis V., Caldara M. & Pennetta L. (2014a) - *The marine and alluvial terraces of Tavoliere di Puglia plain (southern Italy)*. Journal of Maps, **10**(1), 114-125.

De Santis V., Caldara M. & Pennetta L. (2020a) - *Continuous backstepping of Holocene coastal barrier systems into incised valleys: Insights from the Ofanto and Carapelle-Cervaro valleys*. Water, **12**(6), 1799.

De Santis V., Caldara M. & Pennetta L. (2020b) -*Transgressive architecture of coastal barrier systems in the Ofanto incised valley and its surrounding shelf in response to stepped sea-level rise*. Geosciences, **10**(12), 497.

De Santis V., Caldara M., Pennetta L., Torres T. & Ortiz J.E. (2013) - *Unconformity Bounded Stratigraphic Units in an Italian alluvial plain area: recognising and dating*. Journal of Sedimentary Research, **83**, 96-114.

De Santis V., Caldara M., Torres T. & Ortiz J.E. (2014b) - *Two middle Pleistocene warm stages in the Terraced Deposits of the Apulia Region (southern Italy)*. Quaternary international, **332**, 2-18.

De Santis V., Caldara M., Torres T. & Ortiz J.E. (2010) - *Stratigraphic units of the Apulian Tavoliere Plain: chronology, correlation with marine isotope stages and implication regarding vertical movements*. Sedimentary Geology, **228**, 255-270.

De Santis V., Caldara M., Torres T., Ortiz J.E. & Sánchez-Palencia Y. (2018) - *A review of MIS 7 and MIS 5 terrace deposits along the gulf of Taranto based on new stratigraphic and chronological data*. Italian Journal of Geosciences, **137**, 349-368.

De Santis V., Caldara M., Torres T., Ortiz J.E. & Sánchez-Palencia Y. (2020c) - *The role of beach ridges, spits, or barriers in understanding marine terraces processes on loose or semiconsolidated substrates: Insights from the givoni of the Gulf of Taranto (southern Italy)*. Geological Journal, **55**(4), 2951-2975.

De Santis V., Scardino G., Ortiz J.E., Sánchez-Palencia Y. & Caldara M. (2021) - *Pleistocene terracing phases in the metropolitan area of Bari - AAR dating and deduced uplift rates of the Apulian foreland*. Rendiconti Online della Società Geologica Italiana, **54**, 49-61, https://doi.org/10.3301/ROL.2021.03.

Doglioni C., Mongelli F. & Pieri P. (1994) - *The Puglia uplift (SE Italy): an anomaly in the foreland of the Apenninic subduction due to buckling of a thick continental lithosphere*. Tectonics, **13**(5), 1309-1321.

Doglioni C., Tropeano M., Mongelli F. & Pieri P. (1996) - *Middle-late Pleistocene uplift of Puglia: an anomaly in the Apenninic foreland*. Memorie Società Geologica Italiana, **51**, 101-117.

Düsterhus A., Tamisiea M. E. & Jevrejeva S. (2016) - *Estimating the sea level highstand during the Last Interglacial: a probabilistic massive ensemble approach*. Geophysical Journal International, **206**, 900-920.

Dutton A., Carlson A.E., Long A.J., Milne G.A., Clark P.U., De Conto R., Horton B.P., Rahmstorf S. & Raymo M.E. (2015) - *Sea-level rise due to polar ice-sheet mass loss during past warm periods*. Science, **349**(6244), aaa4019.

Evelpidou N, Vassilopoulos A. & Pirazzoli P.A. (2012) - *Holocene emergence in Euboea Island (Greece)*. Marine Geology, **295-298**, 14-19

Faccenna C., Becker T.W., Miller M.S., Serpelloni E. & Willett S.D. (2014) - *Isostasy, dynamic topography, and the elevation of the Apennines of Italy*. Earth and Planetary Science Letters, **407**, 163-174.

Faccenna C., Funiciello F., Civetta L., D'antonio M., Moroni M. & Piromallo C. (2007) - *Slab disruption, mantle circulation and the opening of the Thyrrenian basin*. Geological Society of America Special paper, **418**, 153-169.

Faccenna C., Molin P., Orecchio B., Olivetti V., Bellier O., Funiciello F., Minelli L., Piromallo C. & Billi A. (2011) - *Topography of the Calabria subduction zone (southern Italy): Clues for the origin of Mt. Etna*. Tectonics, **30**(1), 1-20.

Ferranti L., Antonioli F., Mauz B., Amorosi A., Dai Pra G., Mastronuzzi G., Monaco C., Orru P., Pappalardo M., Radtke U., Renda P., Romano P., Sansò P. & Verrubbi V. (2006) - *Markers of the last interglacial sea-level high stand along the coast of Italy: tectonic implications*. Quaternary International, **145-146**, 30-54.

Ferranti L., Burrato P., Sechi D., Andreucci S., Pepe F. & Pascucci V. (2021) - *Late Quaternary coastal uplift of southwestern Sicily, central Mediterranean Sea*. Quaternary Science Reviews, **255**, 106812.

Ferranti L. & Oldow J.S. (2006) - *Rates of late Neogene deformation along the southwestern margin of Adria, southern Apennines orogen, Italy*. In: Pinter N., Gyula G., Weber J., Stein S., Medak D. (eds) *The Adria Microplate: GPS Geodesy, Tectonics and Hazards*. Nato Science Series: IV: Earth and Environmental Sciences, **61**. Springer, Dordrecht.

Fiorini A., Curci A., Spinapolice E.E. & Benazzi S. (2019) - *Grotta di Uluzzo C (Nardò-Lecce): risultati preliminari, strumenti e metodi dell'indagine archeologica*. The Journal of Fasti Online, www.fastionline.org/docs/FOLDER-it-2019-440.pdf.

Flessa K.W., Cutler A.H. & Meldahl K.H. (1993) - *Time and taphonomy: quantitative estimates of time-averaging and stratigraphic disorder in a shallow marine habitat*. Paleobiology, **19**(2), 266-286.

Gignoux M. (1913) - *Les formations marines: Pliocènes et Quaternaires de l'Italie du sud et de la Sicile*. A. Rey; J.-B. Baillière, Lyon; Paris

Grant K.M., Rohling E.J, Ramsey C.B., Cheng H., Edwards R.L., Florindo F., Heslop, D., Marra F., Roberts A.P., Tamisiea M.E. & Williams F. (2014) - *Sea-level variability over five glacial cycles*. Nature Communications, **5**, 5076.

Hearty P.J. (1988) - *An inventory of last interglacial (s.l.) age deposits from the Mediterranean basin: A study of isoleucine epimerization and U-series dating*. Zeitschriji fur Geomorphologie, Suppl.-Bd., *62*, 51- 69.

Hearty P.J. (1987) - *New data on the Pleistocene of Mallorca*. Quaternary Science Reviews, **6**, 245-257.

Hearty P.J. & Dai Pra G. (1985) - *Aminostratigraphy and Th^{230}/U^{234} - U dating of Quaternary shoreline in the Puglia region of southern Italy*. Proceedings of the Fifth International Coral Reef Congress, Papeete, Tahiti, May 1985, 163-169.

Hearty P.J. & Dai Pra G. (1987) – *Paleogeographic reconstruction of Quaternary environments in Toscan a and north Lazio, central Italy*. Bollettino del Servizio Geologico d'Italia, **106**, 189-224.

Hearty P.J. & Dai Pra G. (1992) - *The age and stratigraphy of Middle Pleistocene and younger deposits along the Gulf of Taranto (Southeast Italy)*. Journal of Coastal Research, **8**(4), 82-105.

Hearty P.J.; Hollin J.T. & Dumas B. (1987). *Geochronology of Pleistocene littoral deposits on the Alicante and Almeria coasts of Spain*. In: C. Zazo (Eds.), *Late Quaternary Sea Level Changes in Spain*. Trab. Neogeno-Cuaternario, **10**, 95-105.

Hearty P.J., Hollin J.T., Neumann A.C., O'Leary M.J. & Mcculloch M. (2007) - *Global sea-level fluctuations during the Last Interglaciation (MIS 5e)*. Quaternary Science Reviews, **26**, 2090-2112.

Hearty P.J., Miller G., Stearns C. & Szabo B.J. (1986) - *Aminostratigraphy of Quaternary shorelines in the Mediterranean basin*. Geological Society of America Bulletin, **97**, 850-858.

Kaufman D.S. (2000) - Amino acid racemization in ostracodes, in Goodfriend, G., Collins, M., Fogel, M., Macko, S., and Wehmiller, J., eds, Perspectives in Amino Acid and Protein Geochemistry: New York, Oxford University Press, p. 145–160.

Kaufman D.S. & Manley W.F. (1998) - *A new procedure for determining DL amino acid ratios in fossils using reverse phase liquid chromatography*. Quaternary Science Reviews, **17**, 987-1000.

Kidwell S.M. (1998) - *Time-averaging in the marine fossils record: overview of strategies and uncertainties*. Geobios **30**(7), 977-995.

Kopp R.E., Simons F.J., Mitrovica J.X., Maloof A.C. & Oppenheimer M. (2009) - *Probabilistic assessment of sea level during the last interglacial stage*. Nature, **462**, 863-867.

Kopp R.E., Simons F.J., Mitrovica J.X., Maloof A.C. & Oppenheimer M. (2013) - *A probabilistic assessment of sea level variations within*

the last interglacial stage. Geophysical Journal International, **193**, 711-716.

Kowalewski M. (1997) - *The reciprocal taphonomic model*. Lethaia, **30**, 86-88.

Iannone A. & Pieri P. (1979) - *Considerazioni critiche sui tufi calcarei delle Murge. Nuovi dati litostratigrafi ci e paleoambientali*. Geografia Fisica e Dinamica Quaternaria, **2**, 173-186.

Largaiolli T., Martinis B., Mozzi G., Nardin M., Rossi D. & Ungaro S. (1969) - *Note illustrative del della Carta Geologica d'Italia alla scala 1:100.000, F. 214 "Gallipoli"*. Servizio Geologico d'Italia, Roma.

Lavecchia G, Boncio P, Creati N. & Brozzetti F. (2003) - *Some aspects of the Italian geology not fitting with a subduction scenario*. Journal of the Virtual Explorer, **10**, 1-14.

Lorscheid T, Stocchi P, Casella E., Gómez-Pujol L., Vacchi M., Mann T. & Rovere A. (2017) - *Paleo sea-level changes and relative sea-level indicators: Precise measurements, indicative meaning and glacial isostatic adjustment perspectives from Mallorca (Western Mediterranean)*. Palaeogeography, Palaeoclimatology, Palaeoecology, **473**, 94-107

Marra F., Florindo F., Anzidei M. & Sepe V. (2016). *Paleo-surfaces of glacio-eustatically forced aggradational successions in the coastal area of Rome: assessing interplay between tectonics and sea-level during the last ten interglacials*. Quaternary Science Review, **148**, 85-100.

Marra F., Bahain J.J., Jicha B.R., Nomade S., Palladino D.M., Pereira A., Tolomei C., Pierre Voinchet P., Anzidei M., Aureli D., Ceruleo P., Falgueres C., Florindo F., Gatta M., Ghaleb B., La Rosa M., Peretto C., Petronio C., Rocca R., Rolfo M.F., Salari L., Smedile A. & Tombret O. (2019) - *Reconstruction of the MIS 5.5, 5.3 and 5.1 coastal terraces in Latium (central Italy): A re-evaluation of the sea-level history in the Mediterranean Sea during the last interglacial*. Quaternary International, **525**, 54-77.

Marra F., Rolfo F.M., Gaeta M. & Florindo F. (2020) - *Anomalous Last Interglacial Tyrrhenian sea levels and Neanderthal settling at Guattari and Moscerini caves (central Italy)*. Scientific Reports, **10**, article n.11929. https://doi.org/10.1038/s41598-020-68604-z.

Marsico A., Selleri A., Mastronuzzi G., Sansò P. & Walsh N. (2003) - Cyptokarstr a case-study of the Quaternary landforms of southern Apulia (southern Italy). Acta Carsologica, **32**(2), 147-159.

Medina-Elizade M. (2013) - *A compilation of coral sea-level beenchmarks: Implications and new challenges*. Earth and Planetary Science Letters, **362**, 310-318.

Mastronuzzi G., Caputo R., Bucci D., Fracassi U., Iurilli V., Milella M., Pignatelli C., Sansò P. & Selleri G. (2011) - *Middle-Late Pleistocene evolution of the Adriatic coastline of Southern Apulia (Italy) in response to relative sea-level changes*. Geografia Fisica e Dinamica Quaternaria, **34**(2), 207-221.

Mastronuzzi G., Quinif Y., Sansò P. & Selleri G. (2007) - *Middle-Late Pleistocene polycyclic evolution of a geologically stable coastal: area (southern Apulia, Italy)*. Geomorphology, **86**, 393-408.

Mastronuzzi G. & Sansò P. (Eds.) (2003) - *Quaternary coastal morphology and sea level changes. Field Guide. Puglia 2003, Final Conference –Project IGCP 437 UNESCO – IUGS*, Otranto/Taranto – Puglia (Italy) 22– 28 September 2003, GI2S Coast – Gruppo Informale di Studi Costieri, Research Publication, **5**, 184 pp, Brizio srl, Taranto.

Meldahl K.H., Flessa K.W. & Cutler A.H. (1997) - *Time-averaging and postmortem skeletal survival in benthic fossil assemblages: quantitative comparisons among Holocene environments*. Paleobiology, **23**, 209-229.

Meschis M., Roberts G. P., Robertson J. & Briant R.M. (2018) - *The relationships between regional Quaternary uplift, deformation across active normal faults, and historical seismicity in the upper plate of subduction zones: the Capo D'Orlando fault. NE Sicily*. Tectonics, **37**(5), 1231-1255.

Meschis M., Scicchitano G., Roberts GP., Robertson J., Barreca G., Monaco C., Spampinato C., Sahy D., Antonioli F., Mildon Z.K. & Scardino G. (2020) - *Regional deformation and offshore crustal local faulting as combined processes to explain uplift through time constrained by investigating differentially uplifted late quaternary paleoshorelines: the Foreland Hyblean Plateau, SE Sicily*. Tectonics, **39**: e2020TC006187. https://doi.org/10.1029/2020TC006187.

Murray-Wallace C.V. & Woodroffe C.D. (2014) - *Quaternary Sea-Level Changes: A Global Perspective*. Cambridge University Press.

Negri A., Amorosi A., Antonioli F., Bertini A., Florindo F., Lurcock P.C., Marabini S., Mastronuzzi G., Regattieri E., Rossi V., Scarponi D., Taviani M., Zanchetta G. & Vai G.B. (2015) - *A potential global boundary stratotype section and point (GSSP) for the Tarentian Stage, Upper Pleistocene, from the Taranto area (Italy): Results and future perspectives*. Quaternary International, **383**, 145-157.

O'Leary M., Hearty P., Thompson W., Raymo M.E, Mitrovica J.X. & Webster J.M. (2013) - *Ice sheet collapse following a prolonged period of stable sea level during the last interglacial*. Nature Geosciences, **6,** 796-800.

Ortiz J.E., Torres T., González-Morales M.R., Abad J., Arribas I., Fortea F. J., García-Belenguer F. & Gutiérrez-Zugasti I. (2009) - *The aminochronology of man-induced shell middens in caves in Northern Spain*. Archaeometry, **51**, 123-139.

Ortiz J.E., Gutiérrez-Zugasti I., Torres T., González-Morales M. & Sánchez-Palencia Y. (2015) - *Protein diagenesis in Patella shells: implications for amino acid racemisation dating*. Quaternary Geochronology, **27**, 105-118.

Palmentola G. & Lazzari M. (2005) - *Proposal for a thematic itinerary on geomorphological sites along the western coast of the Salento peninsula, southern Italy*. Italian Journal of Quaternary Sciences, **18**(1), 115-123.

Pedoja K., Jara-Muñoz J., De Gelder G., Robertson J., Meschis M., Fernandez-Blanco D., Nexer M., Poprawski Y., Dugué O., Delcaillau B., Bessin P., Benabdelouahed M., Authemayou C., Husson L., Regard V., Menier D. & Pinel B. (2018) - *Neogene-Quaternary slow coastal uplift of western Europe through the perspective of sequences of strandlines from the Cotentin Peninsula (Normandy, France)*. Geomorphology, **303**, 338-356.

Pirazzoli P.A., Stiros S.C., Arnold M., Laborel J. & Laborel-Deguen F. (1999) - *Late Holocene coseismic vertical displacements and tsunami deposits near Kynos, Gulf of Euboea, Central Greece*. Physics and Chemistry of the Earth, Part A: Solid Earth and Geodesy, **24**, 361-367.

Ricchetti G. & Ciaranfi N. (2013) - *Note Illustrative della Carta Geologica d'Italia alla scala 1:50.000, F. 536 Ugento*. 120 pp., LAC, Firenze.

Ricchetti G., Ciaranfi N., Luperto Sinni E., Mongelli F., Pieri P. (1992) - *Geodinamica ed evoluzione sedimentaria e tettonica dell'avampaese apulo*. Memorie Società Geologica Italiana, **41**(1988), 57-82.

Ricchetti G. & Mongelli F. (1980) - *Flessione e campo gravimetrico della micropiastra apula*. Bollettino della Società Geologica Italiana, **99**, 431-436.

Roberts G.P., Houghton S.L., Underwood C., Papanikolaou I., Cowie P.A., van Calsteren P., Wigley T., Cooper F.J. & McArthur J.M. (2009) - *Localization of quaternary slip rates in an active rift in 105 years: An example from central Greece constrained by 234U- 230Th coral dates from uplifted paleoshorelines*. Journal of Geophysical Research, **114**, B10406.

Roberts G. P., Meschis M., Houghton S., Underwood C. & Briant R.M. (2013) - *The implications of revised Quaternary palaeoshoreline chronologies for the rates of active extension and uplift in the upper plate of subduction zones*. Quaternary Science Reviews, **78**, 169-187.

Robertson J., Meschis M., Roberts G. P., Ganas A. & Gheorghiu D.M. (2019) - *Temporally constant quaternary uplift rates and their relationship with extensional upper-plate faults in south Crete (Greece), constrained with ^{36}CL cosmogenic exposure dating*. Tectonics, **38**(4), 1189-1222.

Rohling E., Grant K., Hemleben C., Siddal M., Hoogakker B. A. A., Bolshaw M. & Kucera M. (2008) - *High rates of sea-level rise during the last interglacial period*. Nature Geosciences, **1**, 38-42.

Rohling E.J., Foster G.L., Grant K.M., Marino G., Roberts A.P., Tamisiea M.E. & Williams F. (2014) - *Sea-level and deep-sea-temperature variability over the past 5.3 million years*. Nature, **508**(7497), 477-482.

Rohling E.J., Hibbert F.D., Grant K.M., Galaasen E.V., Irvali N., Kleiven H.F., Marino G., Ninnemann U., Roberts A.P., Rosenthal Y. & Schulz H. (2019) - *Asynchronous Antarctic and Greenland ice-volume contributions to the last interglacial sea-level highstand*. Nature Communications, **10**(1), 5040.

Rovere A., Raymo M.E., Vacchi M., Lorscheid T., Stocchi P., Gómez-Pujol L., Harris D.L., Casella E., J. O'Leary M. & Hearty P.J. (2016) - *The analysis of Last Interglacial (MIS 5e) relative sea-level indicators: Reconstructing sea-level in a warmer world*. Earth-Science Reviews, **159**, 404-427

Sansò P., Margiotta S., Mastronuzzi G. & Vitale A. (2015) - *The geological heritage of salento leccese area (Apulia, southern Italy)*. Geoheritage, **7**, 85-101.

Siddall M., Rohling E., Almogi-Labin A., Hemleben C., Meischner D., Schmelzer I. & Smeed D.A. (2003) - *Sea-level fluctuations during the last glacial cycle.* Nature, **423**, 853-858.

Stiros S.C., Arnold M., Pirazzoli P.A., Laborel J., Laborel F. & Papageorgiou S. (1992) - *Historical coseismic uplift on Euboea Island, Greece*. Earth and Planetary Science Letters, **108**, 109-117.

Taviani M. (2014) - *Unpersisting Persististrombus: a Mediterranean story*. Vieraea, **42**, 9-18

Torres T., Llamas J.F., Canoira L., Coello J., García-Alonso P. & Ortiz J.E. (2000) - *Aminostratigraphy of two marine sequences from the Mediterranean coast of Spain. Cabo de Huertas (Alicante) and Garrucha (Almería)*. In: Goodfriend G.A., Collins M.J., Fogel M.L., Macko S.A., Wemiller J.F. (Eds.), *Perspectives in Amino Acid and Protein Geochemistry*. Oxford University Press, New York, 263-278.

Torres T., Ortiz J.E. & Arribas I. (2013) - *Variations in racemization/epimerization ratios and amino acid content of Glycymeris shells in raised marine deposits in the Mediterranean*. Quaternary Geochronology, **16**, 35-49.

Torres, T., Ortiz, J.E., Arribas, I., Delgado, A., Julià, R., Martín-Rubí, J.A. (2010) - *Geochemistry of Persististrombus latus Gmelin from the Pleistocene Iberian realm*. Lethaia, **43**, 143-163.

Tozzi M. (1993) - Assetto tettonico dell'Avampaese Apulo meridionale (Murge meridionali-Salento) sulla base dei dati strutturali. Geologica Romana, **29**, 95-111.

Tropeano M., Sabato L. & Pieri P. (2002) - *Filling and cannibalization of a foredeep: the Bradanic Trough, Southern Italy*. Geological Society, London, Special Publications, **191**, 55-79.

Vacchi M., Marriner N., Morhange C., Spada G., Fontana A. & Rovere A. (2016) – *Multiproxy assessment of Holocene relative sea-level changes in the western Mediterranean:Sea-level variability and improvements in the definition of the isostatic signal*. Earth Science Reviews, **155**, 172-197.

Valenzano E., Scardino G., Cipriano G., Fago, P., Capolongo D., De Giosa F., Lisco S., Mele D., Moretti M. & Mastronuzzi G. (2018) - *Holocene morpho-sedimentary evolution of the Mar Piccolo basin (Taranto, Southern Italy)*. Geografia Fisica e Dinamica Quaternaria, **41**, 119-135

Van Hinsbergen D.J.J., Mensink M., Langereis C.G., Maffione M., Spalluto L., Tropeano M., Sabato L. (2014) - *Did Adria rotate relative to Africa?* Solid Earth, **5**, 611-629.

Van Hinsbergen D.J.J., Torsvik T.H., Schmid S.M., Maţenco L.C., Maffione M., Vissers R.L.M., Gürer D. & Spakman W. (2020) - *Orogenic architecture of the Mediterranean region and kinematic reconstruction of its tectonic evolution since the Triassic*. Gondwana Research, **81**, 79-229.

Vicens D., Gràcia F. & Ginés A. (2012) - *Quaternary beach deposits in Mallorca: paleontological and geomorphological data*. In: Ginés A., Ginés J., Gómez-Pujol L., Onac B.P., Fornós J.J. (Eds.), *Mallorca: A Mediterranean Benchmark for Quaternary Studies*. Monografies de la Societat d'Història Natural de les Balears, 55-83.

Waelbroeck C., Labeyrie L., Michel E., Duplessy J.C., Mcmanu J.F., Lambeck K., Balbon E., Labracherie M. (2002) - *Sea-level and deep water temperature changes derived from benthic foraminifera isotopic records*. Quaternary Science Reviews, **21**, 295-305.

Westaway R. (1993) - *Quaternary uplift of southern Italy*. Journal of Geophysical Research, **98**(B12), 741-772.

Zander A., Fülling A., Brückner H. & Mastronuzzi G. (2006) - *OSL dating of Upper Pleistocene littoral sediments: a contribution to the chronostratigraphy of raised marine terraces bordering the Gulf of Taranto, South Italy*. Geografia Fisica e Dinamica Quaternaria, **29**(1), 33-50.

Zazo C., Goy J.L., Dabrio C.J., Bardajì T., Hillaire-Marcel C., Ghaleb B., Gonzaɑlez-Delgado J.A. & Soler V. (2003) - *Pleistocene raised marine terraces of the Spanish Mediterranean and Atlantic coasts: records of coastal uplift, sea-level highstands and climate changes*. Marine Geology, **194**, 103-133.

Zazo C., Goy J.L., Dabrio C.J., Lario J., González-Delgado J.A., Bardají T., HillaireMarcel C., Cabero A., Ghaleb B., Borja F., Silva P.G., Roquero E. & Soler V. (2013) - *Retracing the Quaternary history of sea-level changes in the Spanish Mediterranean-Atlantic coasts: geomorphological and sedimentological approach*. Geomorphology, **196**, 36-49.

Manuscript received 13 March 2021; accepted 27 June 2021; published online XX June 2021;
editorial responsibility and handling by O. Vaselli.